UNCLASSIFIED

AD 297 044

Reproduced
by the

ARMED SERVICES TECHNICAL INFORMATION AGENCY
ARLINGTON HALL STATION
ARLINGTON 12, VIRGINIA

UNCLASSIFIED

NOTICE: When government or other drawings, specifications or other data are used for any purpose other than in connection with a definitely related government procurement operation, the U. S. Government thereby incurs no responsibility, nor any obligation whatsoever; and the fact that the Government may have formulated, furnished, or in any way supplied the said drawings, specifications, or other data is not to be regarded by implication or otherwise as in any manner licensing the holder or any other person or corporation, or conveying any rights or permission to manufacture, use or sell any patented invention that may in any way be related thereto.

N-63-2-5

CATALOGED BY ASTIA
AS AD No 297044

Office of Naval Research

Contract Nonr-1866 (32) NR 371-016

THEORY OF RADIALLY STRATIFIED MEDIA

PART I. THE BICONICAL ANTENNA IN A RADIALLY STRATIFIED MEDIUM

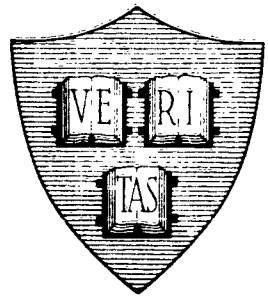

By

John G. Fikioris

January 2, 1963

Technical Report No. 390

Cruft Laboratory
Harvard University
Cambridge, Massachusetts

297 044

Office of Naval Research

Contract Nonr-1866(32)

NR - 371 - 016

Technical Report

on

THEORY OF RADIALLY STRATIFIED MEDIA

Part I. The Biconical Antenna in a Radially Stratified Medium

by

John G. Fikioris

January 2, 1963

The research reported in this document was supported by Grant 20225 of the National Science Foundation. Publication was made possible through support extended Cruft Laboratory, Harvard University, by the Navy Department (Office of Naval Research), the Signal Corps of the U. S. Army, and the U. S. Air Force under ONR Contract Nonr-1866 (32). Reproduction in whole or in part is permitted for any purpose of the United States Government.

Technical Report No. 390

Cruft Laboratory

Harvard University

Cambridge, Massachusetts

PREFACE

The numerical computations were done at the Computation Center at MIT, Cambridge, Massachusetts.

The author wishes to thank the staff of the Center for their generous allotment of computer time and its further extensions that, inevitably, became necessary.

Mr. E. Rising and his assistants for drawing all the figures.

His wife for typing the first draft and for her unfailing encouragement during the long months that the research was under way.

Professor T. T. Wu and Dr. Seshadri for useful discussions and suggestions.

His fellow students whose interest in this work and truly academic spirit made research at Harvard an unforgettable experience.

And finally Professor R. W. P. King whose advice and continuous encouragement made the completion of the thesis possible.

TABLE OF CONTENTS

Page

LIST OF FIGURES *

* All figures, except the last, are found at the end of their respective chapters.

SYNOPSIS

Electromagnetic fields in inhomogeneous and dissipative media have attracted considerable attention. Such media are characterized in general by a dielectric constant ϵ and a conductivity σ that vary with the coordinates x, y, z. Examples are to be found in the field of inhomogeneous plasma, in underwater communication, in E. M. lenses and in a study of antennas used as probes in such media.

This research is restricted to radially stratified media with $\epsilon = \epsilon(r)$, $\sigma = \sigma(r)$, where r is the radial distance in spherical coordinates. In these coordinates Maxwell's equations are still separable if the complex dielectric factor $\xi = \epsilon - i\sigma/\omega = \epsilon_o f(r)$ depends only on r. The angular equation is not affected. However, the radial equation is no longer the spherical Bessel equation of the homogeneous case. Its coefficients depend on the "stratification function" f(r) and contain additional singularities in the complex r-plane. The biconical antenna is the most general problem that can be encountered; it requires the solution of the complicated radial equation from r=0 to r=∞. The theory, nevertheless, is readily applicable to all electromagnetic problems arising in the presence of such media.

For the stratification function f(r) the following form was considered: $f(r) = (r+a)/(r+b)$, where a and b are constants, in general complex. Even this simple dependence introduces two new finite singularities in the radial differential equation beyond the usual singularities at r=0 and r=∞. Furthermore, it has been proved that the analysis can readily be extended to more general types of f(r).

The antenna problem requires the analytical solution of the radial wave equation inside and outside the antenna and the matching of the E. M. fields across the spherical surface

containing the antenna. Series solutions $R_1(x)$, $R_2(x)$ around $x=0$ and asymptotic solutions $R_3(x)$, $R_4(x)$ around $x=\infty$ of the second-order differential equation are found first. For computational purposes and, mainly, for reasons of matching the linear connecting formulas between the two sets of solutions (around $x=0$ and $x=\infty$) of the equation must be found. They provide the analytic continuation of $R_3(x)$, $R_4(x)$ in the vicinity of $x=0$ and the asymptotic expansions of $R_1(x)$, $R_2(x)$ for large $|x|$. The constant coefficients of the linear connecting formulas are found by solving the associated difference equation and its adjoint.

A generalization of Ford's method (reference 7 in the BIBLIOGRAPHY), concerning the asymptotic expansions of solutions of differential equations with polynomial coefficients and with three or more regular singular points and one irregular at infinity, was arrived at. It was then extended to the special but important case of integral values for the difference of exponents of the differential equation, thus providing the complete asymptotic expansion of the second, logarithmic solution of the equation. Explicit formulas for the evaluation of the constant coefficients of these expansions have been developed; each coefficient depends only on a single solution of the adjoint difference equation associated with the original differential equation.

Numerical computations were performed on an IBM 7090 computer. Six different cases of stratified media were considered, five of them dealing with dissipative media. In each case the input impedance of the biconical antenna $Z_1 = R_1 + iX_1$ was computed and plotted for eight different cone angles: $1/20^\circ$, $1/4^\circ$, 1°, 2°, 30°, 39.23°, 55°, 70°. The electrical length of the antenna was varied from 0 to 7 (in certain cases up to 9 or 11).

Concerning the antenna, all effects of dissipation and stratification, expected on physical grounds and observed experimentally for dipole antennas, were clearly exhibited. General conclusions could be drawn regarding the behaviour of the antenna

in such media by mere inspection and comparison of the graphs in different cases.

From the mathematical point of view the results of the computations completely verified the theory and established its capability to yield accurate numbers. In the overlapping region between convergent and asymptotic series representations, agreement of 4, even 5, decimals was obtained, with single precision (8-decimal) arithmetic. The coefficients of the asymptotic expansions were computed with an accuracy of 4 to 6 decimals.

PART I

THE BICONICAL ANTENNA IN A RADIALLY STRATIFIED MEDIUM

CHAPTER 1

FORMULATION OF THE PROBLEM

INTRODUCTION

This research is concerned with the solution of the following specific problem :

" The behaviour of a biconical antenna immersed in a radially and continuously stratified medium."

It should be emphasized from the start, however, that the investigation is by no means restricted to the biconical antenna. Primarily, it is concerned with the theory of radially and continuously stratified media and can be readily applied to all electromagnetic problems arising in the presence of such media. Examples: Radially stratified electromagnetic lens, E.M. wave propagation in such media, scattering by a spherical object itself radially stratified, etc. In this connection, it can be observed that the biconical antenna is the most general problem; in the following sense: It requires the solution of the differential equation for the radial function in the whole interval $0 \leqq r \leqq \infty$, when, as assumed here, the stratification extends from $r = 0$ to $r = \infty$. It will be seen that this leads to the necessity of determining asymptotic expansions for the solutions of the radial equation valid in the neighborhood of

r=0, not simply for reasons of computation but mainly because of the problem of matching. In contrast, such complications do not arise in a lens problem for example. C. T. Tai, in his paper on Luneberg lens (1 pp. 123-124), obtains a series solution for the radial function convergent for $\rho \leqq 2\rho_a$ while the values of ρ, in this case, never exceed ρ_a. So, the series solution around $\rho=0$ is completely adequate. For the biconical antenna, however, we essentially need the analytic continuation of the solutions in the whole interval $0 \leqq r \leqq \infty$. These statements will become clear later in the paper and in the course of developing the theory.

It can be argued at this point that the biconical antenna does not require the solution of the radial equation for TE waves, since only TM and TEM waves are involved. It will be seen, however, that the differential equation for the radial TM function is more general than the equation corresponding to TE waves. After obtaining these equations, a discussion relative to this point will be included.

As a general outline, the paper is divided into two PARTS. In PART I, Chapter 1 deals with the formulation of the problem; Chapter 2 with the specific problem of a biconical antenna in a radially stratified medium; Chapter 3 includes and discusses numerical results obtained in a number of cases. The complete mathematical analysis is developed in PART II, divided into three chapters. In Chapter 1 series expansions of the functions involved are obtained; Chapter 2 is concerned with their asymptotic expansions and Chapter 3 contains remarks relative to the theory developed in the previous chapters as well as possible generalizations.

The complexity of the problem depends exclusively on the "stratification function" f(r), where

$$\epsilon(r) = \epsilon f(r) \quad , \quad \kappa^2(r) = \omega^2 \mu \epsilon(r) = \kappa^2 f(r) \qquad (1\text{-}1)$$

Solutions have been obtained in various cases for certain simple

functions $f(r)$ and can be found in the literature. Many of them are mentioned in references 1 and 2 in the BIBLIOGRAPHY. This research is also concerned with a simple form for $f(r)$. It represents a type of variation shown in figure (1-1). $f(r)$ starts from finite values, greater or less than 1, at $r=0$ and continuously approaches the value 1 at $r=\infty$. It will be seen that such a form is more general and more complicated than all cases considered up to the present. On the other hand, a variation such as the one shown in figure (1-1), so loosely defined by the above requirements, can be represented by an infinite number of functional forms. Unfortunately, complete solutions can not be obtained in the general case. Here, one of the simplest forms for $f(r)$ was chosen, satisfying the above requirements. Namely:

$$f(x) = \frac{x+a}{x+b} = 1 + \frac{c}{x+b} , \qquad (1-2)$$

where a,b are constant parameters, in general complex, and

$$c = a-b . \qquad (1-3)$$

A complete solution of the problem was obtained in this case. The parameters a and b provide $f(r)$ with the flexibility to fit a great number of variations in accordance with the requirements of figure (1-1). And, most important, despite this severe restriction on the form of $f(r)$, the analysis that follows permits an insight into the complexity of the problem and the type of complications that are introduced as $f(r)$ becomes more complicated and general in form. In fact, it will be seen that the analysis of this case is readily applicable to three other types of $f(r)$ of a similar functional form. Furthermore, the analysis shows by itself what kind of generalizations in the form of $f(r)$ can be introduced without rendering the method of solution inapplicable. Discussions, relative to these statements, are given at the appropriate stages of the analysis.

MAXWELL'S EQUATIONS IN A RADIALLY STRATIFIED MEDIUM

In the time periodic case with assumed time dependence $e^{i\omega t}$ and in a radially stratified and generally dissipative medium, Maxwell's equations are:

$$\nabla \times \bar{E} = -i\omega\mu\bar{H} \tag{1-4}$$

$$\nabla \times \bar{H} = i\omega\xi(r)\bar{E} \tag{1-5}$$

The boundary conditions between the medium and a perfect conductor (in which $\bar{E}_c = \bar{B}_c = 0$)are (3 p. 366):

$$\hat{n} \times \bar{E} = 0 \tag{1-6}$$

$$\hat{n} \cdot \bar{H} = 0 \, . \tag{1-7}$$

μ, the absolute permeability of the medium, is considered real and constant. ξ , the complex dielectric factor, is given by (3 p. 366):

$$\xi = \epsilon(1-i\sigma/\omega\epsilon) = \epsilon - i\sigma/\omega \tag{1-8}$$

and is here considered to be a function of the radius r. Thus $\xi = \xi(r)$. More specific definitions will be given later.

We now express Maxwell's equations (1-4),(1-5) in spherical coordinates r,θ,ϕ . If variations with respect to ϕ are not involved, i.e. if $\frac{\partial}{\partial\phi} = 0$, we obtain:

$$\frac{\partial}{\partial\theta}(\sin\theta\, E_\phi) = -i\omega\mu r\sin\theta\, H_r \tag{1-9}$$

$$\frac{\partial}{\partial r}(rE_\phi) = i\omega\mu r H_\theta \tag{1-10}$$

$$\frac{\partial}{\partial r}(rE_\theta) - \frac{\partial E_r}{\partial\theta} = -i\omega\mu r H_\phi \tag{1-11}$$

$$\frac{\partial}{\partial\theta}(\sin\theta\, H_\phi) = i\omega\xi(r)\sin\theta\, E_r \tag{1-12}$$

$$\frac{\partial}{\partial r}(rH_\phi) = -i\omega\xi(r) r E_\theta \tag{1-13}$$

$$\frac{\partial}{\partial r}(rH_\theta) - \frac{\partial H_r}{\partial\theta} = i\omega\xi(r) r E_\phi \, . \tag{1-14}$$

The case considered, $\frac{\partial}{\partial \phi} = 0$, corresponds to the specific problem of a straight biconical antenna, placed at the center of the spherically stratified medium, coinciding, naturally, with the origin of the spherical coordinate system r,θ,ϕ as shown in figure (1-2). No loss of generality is introduced by considering this special case. It will be seen in a short while, that the only modification introduced by the radial stratification appears in the radial equation. The angular functions satisfy the same equations, which would be obtained if the medium were considered homogeneous, i.e. if $f(r) \equiv 1$. These results are also valid in the general case of three-dimensional variations; see for example, references 1 and 2, where the equations satisfied by the electromagnetic field associated with a radially stratified medium, are obtained by solving directly the vector wave equation in the most general case. The general analysis verifies the statements made above. Furthermore, it yields the same radial equations for TM, TE and TEM waves as can be obtained by solving the simplified equations (1-9) to (1-14).

These equations separate into two sets. The first, containing equations (1-11),(1-12) and (1-13), involves H_ϕ, E_θ, E_r only and corresponds to TM waves. The second, containing equations (1-9),(1-10),(1-14), involves E_ϕ, H_θ, H_r only and corresponds to TE waves.

<u>TM Spherical Waves:</u> Equations (1-12),(1-13) express E_r and E_θ in terms of H_ϕ. Substituting in (1-11) we obtain:

$$\frac{\partial}{\partial r}\left[\frac{1}{\xi(r)}\frac{\partial}{\partial r}(rH_\phi)\right] + \frac{\partial}{\partial \theta}\left[\frac{1}{\xi(r)}\frac{1}{r\sin\theta}\frac{\partial}{\partial \theta}(\sin\theta\, H_\phi)\right] = -\omega^2 \mu r H_\phi \qquad (1\text{-}15)$$

We now separate the variables:

$$H_\phi(r,\theta) = F(r)\,\Theta(\theta) \qquad (1\text{-}16)$$

and, after division by $\frac{F(r)\Theta(\theta)}{r\,\xi(r)}$, (1-15) becomes:

$$\frac{r\xi(r)}{F(r)}\frac{d}{dr}\left[\frac{1}{\xi(r)}\frac{d}{dr}(rF_{(r)})\right]+\omega^2\mu\,\xi(r)r^2 =$$

$$= -\frac{1}{\Theta(\theta)}\frac{d}{d\theta}\left[\frac{1}{\sin\theta}\frac{d}{d\theta}(\sin\theta\,\Theta_{(\theta)})\right] = \nu(\nu+1)\ ,$$

where $\nu(\nu+1)$ is the separation constant. Calling

$$rF(r) = R(r) \qquad (1\text{-}17)$$

we obtain:

$$\frac{d^2R(r)}{dr^2} - \frac{\xi'(r)}{\xi(r)}\frac{dR(r)}{dr} + \left[\omega^2\mu\,\xi(r) - \frac{\nu(\nu+1)}{r^2}\right]R(r) = 0 \qquad (1\text{-}18)$$

$$\frac{d}{d\theta}\left[\frac{1}{\sin\theta}\frac{d}{d\theta}(\sin\theta\,\Theta_{(\theta)})\right]+\nu(\nu+1)\,\Theta(\theta) = 0\ . \qquad (1\text{-}19)$$

It can be verified immediately that this last equation is satisfied by

$$\Theta(0) = \frac{dT(\theta)}{d\theta}\ , \qquad (1\text{-}20)$$

where $T(\theta)$ is any solution of the Legendre differential equation:

$$\frac{d}{d\theta}(\sin\theta\,\frac{dT}{d\theta})+\nu(\nu+1)\sin\theta\,T(\theta) = 0\ . \qquad (1\text{-}21)$$

We obtain in this manner the following expressions:

$$H_\phi(r,\theta) = \frac{R(r)}{r}\frac{dT}{d\theta} \qquad (1\text{-}22)$$

$$E_\theta(r,\theta) = \frac{i}{\omega}\frac{1}{r\,\xi(r)}\frac{dT}{d\theta}\frac{dR}{dr} \qquad (1\text{-}23)$$

$$E_r(r,\theta) = \frac{i}{\omega}\nu(\nu+1)\frac{R(r)}{r^2\xi(r)}\,T(\theta) \qquad (1\text{-}24)$$

TE Spherical Waves: In a similar way, substituting from (1-9),(1-10) into (1-14) we obtain:

$$\frac{\partial^2}{\partial r^2}(rE_\phi)+\frac{\partial}{\partial\theta}\left[\frac{1}{r\sin\theta}\frac{\partial}{\partial\theta}(\sin\theta\, E_\phi)\right] = -\omega^2\mu\,\xi(r)rE_\phi \quad . \tag{1-25}$$

Separating and following similar steps, we obtain:

$$E_\phi(r,\theta) = \frac{R(r)}{r}\frac{dT}{d\theta} \tag{1-26}$$

$$H_\theta(r,\theta) = -\frac{i}{\omega\mu r}\frac{dT}{d\theta}\frac{dR}{dr} \tag{1-27}$$

$$H_r(r,\theta) = -\frac{i}{\omega\mu}\nu(\nu+1)\frac{R(r)}{r^2}T(\theta) \quad , \tag{1-28}$$

where $T(\theta)$ satisfies again Legendre's equation (1-21), while the equation satisfied by $R(r)$ is:

$$\frac{d^2R(r)}{dr^2}+\left[\omega^2\mu\,\xi(r)-\frac{\nu(\nu+1)}{r^2}\right]R(r) = 0 \quad . \tag{1-29}$$

At this point, we may observe the following: if the stratification involved variations with respect to θ, i.e. if $\xi = \xi(r,\theta)$ - even in the form $\xi = f(r)g(\theta)$ - we would not be able to separate the variables in equations (1-15) and (1-25). It is this essential difficulty which forces us to restrict the problem to radial stratifications.

TEM Spherical Waves: In this case $E_r \equiv H_r \equiv 0$. Being here interested only in the field with circular magnetic lines, we can derive the relations for TEM waves by considering them as a special case of TM waves with $E_r \equiv 0$. Then, from (1-24) we obtain:

$$\nu = 0 \quad , \tag{1-30}$$

while (1-18) and (1-21) become:

$$\frac{d^2R}{dr^2} - \frac{\xi'(r)}{\xi(r)}\frac{dR}{dr} + \omega^2\mu\,\xi(r)\,R(r) = 0 \qquad (1\text{-}31)$$

$$\frac{d}{d\theta}(\sin\theta\,\frac{d\Psi}{d\theta}) = 0 \ .$$

Put now:

$$\frac{d\Psi}{d\theta} = \Psi_o(\theta) \qquad (1\text{-}32)$$

$$R(r) = \frac{dR_o(r)}{dr} \ , \qquad (1\text{-}33)$$

where $R_o(r)$ satisfies the equation:

$$\frac{d^2R_o}{dr^2} + \omega^2\mu\,\xi(r)\,R_o(r) = 0 \ . \qquad (1\text{-}34)$$

Divide by $\xi(r)$ and differentiate with respect to r:

$$\frac{1}{\xi(r)}\frac{d^2R}{dr^2} - \frac{\xi'(r)}{\xi^2(r)dr}\frac{dR}{dr} + \omega^2\mu R(r) = 0 \ ,$$

which is identical with (1-31). Also $\Psi_o(\theta)$ satisfies:

$$\frac{d}{d\theta}(\sin\theta\,\Psi_{o(\theta)}) = 0 \ . \qquad (1\text{-}35)$$

So, with $R_o(r)$ and $\Psi_o(\theta)$ satisfying (1-34) and (1-35) we obtain from (1-22),(1-23),(1-32) and (1-33) the following expressions for the TEM field with circular magnetic lines, i.e. with $H_\theta = 0$:

$$E_r(r,\theta) = 0 \qquad (1\text{-}36)$$

$$E_\theta(r,\theta) = -\,i\omega\mu\,\frac{R_o(r)}{r}\,\Psi_o(\theta) \qquad (1\text{-}37)$$

$$H_\phi(r,\theta) = \frac{1}{r}\frac{dR_o}{dr}\,\Psi_o(\theta) \ . \qquad (1\text{-}38)$$

These expressions and equations (1-34),(1-35) could be

obtained in a more simple way from the original set of Maxwell's equations (1-11) to (1-13) using the fact that in the present case $\bar{E}_r = 0$. The above method was preferred, however, because it shows that, analytically, the TEM field is derivable as a special from the TM wave solutions.

It is clear now that the angular equations (1-21) and (1-35) present no new problem. The problem centers around the solution of the radial equations (1-18),(1-29) and (1-34). The last one is a special case of (1-29), or, through (1-33) and (1-31), a special case of (1-18).

We introduce the electrical radial distance:

$$x = \kappa r \tag{1-39}$$

$$f(r) = f(x/\kappa) = \varphi(x) \tag{1-40}$$

$$\omega^2 \mu \xi(r) = \kappa^2 \varphi(x) \tag{1-41}$$

and equations (1-18),(1-29) and (1-34) become:

$$\text{TM waves :} \quad \frac{d^2R(x)}{dx^2} - \frac{\varphi'(x)}{\varphi(x)} \frac{dR(x)}{dx} + \left[\varphi(x) - \frac{\nu(\nu+1)}{x^2}\right]R(x) = 0 \tag{1-42}$$

$$\text{TE waves :} \quad \frac{d^2R(x)}{dx^2} + \left[\varphi(x) - \frac{\nu(\nu+1)}{x^2}\right] R(x) = 0 \tag{1-43}$$

$$\text{TEM waves :} \quad \frac{d^2R_o(x)}{dx^2} + \varphi(x)\, R_o(x) = 0 \ . \tag{1-44}$$

In a dissipative medium ξ is complex. Then:

$$x = \kappa r = \omega\sqrt{\mu\epsilon}\,[f(h) - ig(h)]r \tag{1-45}$$

takes on complex values in the fourth quadrant of the complex x-plane, from $x=0$ to $x=\infty$. In equation (1-45):

$$h=\sigma/\omega\epsilon \ , \quad f(h)=\cosh\left(\tfrac{1}{2}\sinh^{-1}h\right) \ , \quad g(h)=\sinh\left(\tfrac{1}{2}\sinh^{-1}h\right) \ . \tag{1-46}$$

Tables for f(h) and g(h) can be found in reference 4.

DISCUSSION OF THE RADIAL EQUATIONS

Equation (1-44) for the TEM waves is a special case of (1-42), as it has been explained. It can be solved separately, if it is more convenient to do so.

We consider now equation (1-42) for the TM waves. As it would be expected, in the homogeneous case, i.e. when $\varphi(x) \equiv 1$, it reduces to the spherical Bessel equation:

$$R''(x) + \left[1 - \frac{\nu(\nu+1)}{x^2}\right] R(x) = 0 \quad , \qquad (1\text{-}47)$$

in agreement with established results in this case (5, 6 pp. 7-9). There exists a correspondence between equations (1-47) and (1-42) and it will be pointed out from time to time. Equation (1-47) has a regular singular point at x=0 and an irregular singularity at $x = \infty$ (9 pp. 160-161 168-178 417-428, 10 pp. 58-77). On the other hand, equation (1-42) is much more complicated; in addition to the above mentioned singularities, it has singular points at the singularities of $\varphi(x)$ (or of $\varphi'(x)$) and at the zeros of $\varphi(x)$. The nature of these singularities depends on the nature of the singular points and of the zeros of $\varphi(x)$. We refer, of course, to the complex x-plane when we make these statements. Regarding now equation (1-43) for the TE waves, we observe that, in addition to the singular points at x=0 and $x = \infty$, it has singularities at the singular points of $\varphi(x)$. But the zeros of $\varphi(x)$ are no longer singularities of the equation. So, (1-42) has more singularities than (1-43) - at the zeros of $\varphi(x)$ - and is a more complicated and general differential equation than (1-43) is. At this point, reference to the discussion on page 1-2 can be made. In the specific problem of the biconical antenna,

we are only concerned with TM waves. We consider only equation (1-42), not (1-43), but we treat the more general case.

In accordance with the requirements on $\varphi(x)$ as shown in figure (1-1) and the discussion thereof, we now consider the following special form for $\varphi(x)$:

$$\varphi(x) = \frac{x+a}{x+b} = 1 + \frac{c}{x+b} = f(r) = \frac{\kappa r+a}{\kappa r+b} \qquad (1\text{-}48)$$

$$c = a-b \ , \qquad (1\text{-}49)$$

where a and b are constant parameters.

With the special form of $\varphi(x)$, as given by (1-48), equation (1-42) for TM waves becomes:

$$\frac{d^2R(x)}{dx^2} + \frac{c}{(x+a)(x+b)} \frac{dR}{dx} + \left[1 + \frac{c}{x+b} - \frac{v(v+1)}{x^2}\right] R(x) = 0 \ . \qquad (1\text{-}50)$$

For comparison, equation (1-43) for TE waves reduces in this case to:

$$\frac{d^2R(x)}{dx^2} + \left[1 + \frac{c}{x+b} - \frac{v(v+1)}{x^2}\right] R(x) = 0 \ . \qquad (1\text{-}51)$$

It is obvious now that (1-50) has all the singularities of (1-51) and an additional regular singularity at x=-a. So, the method of obtaining its complete solution can be readily applied to the more simple equation (1-51).

Equation (1-50) has three regular singular points at x=0, x=-a, x=-b and an irregular singularity of the first rank at $x=\infty$ (9 pp. 417-428, 10 pp. 58-77). That is, it possesses two more regular singularities than the Bessel equation (1-47). Problems treated so far in the literature, dealt with "stratification functions" of such simple form, that no additional singularities were introduced in the radial equation. In such cases it is possible to identify the solutions with well-

known functions, for example confluent hypergeometric or Bessel functions with argument dr^m, where d and m are appropriate constants. Tai's paper (1) refers to such cases. Others can be found in references 1 and 2. More complicated cases introducing one more singularity were also treated, but they dealt with situations where the stratification terminates at a finite distance r, for example lens problems. As an example, we cite Tai's paper (1), which also refers to other similar problems treated up to the present time. The comments on page 1-2 reveal the additional difficulties that the biconical antenna presents, when the stratification extends from r=0 to $r=\infty$. We can also see now that a stratification in accordance with the requirements of figure (1-1), even in its simplest form (1-48), introduces at least two more regular singularities into equation (1-50) for TM waves. Later in this paper, Chapter 3, PART II, we shall see how the method of solution can be generalized to more complicated forms for $\varphi(x)$.

Equation (1-50) possesses two independent solutions. Solving the equation around x=0 with the method of Frobenius, we obtain two power series solutions $R_1(x)$ and $R_2(x)$ (defined more precisely in PART II), whose radius of convergence is limited by the nearest to the origin singularity, i.e. valid within the circle $|x|<\min(|a|,|b|)$. By a suitable change of variable, x to t, we can obtain for $R_1(x)$ and $R_2(x)$ power series expressions in terms of t, valid within the circle $|t|<1$, for example, which provide, in the x-plane, the analytic continuation of $R_1(x)$ and $R_2(x)$ outside the circle $|x|<\min(|a|,|b|)$, in fact into the whole half plane of interest where x varies from 0 to ∞. These possibilities will be seen more clearly later, in the course of obtaining explicit solutions to equation (1-50).

Solutions $R_1(x)$ and $R_2(x)$ of (1-50) correspond to the solutions $\sqrt{x}\,J_{\nu+1/2}(x)$ and $\sqrt{x}\,N_{\nu+1/2}(x)$ of equation (1-47),

respectively. Referring to figure (1-2), we observe that in the antenna region (1) we have to use the solution $R_1(x)$ of the radial equation. $R_2(x)$ becomes infinite at x=0. In free space, region (2) in figure (1-2), we must use a third solution $R_4(x)$ of (1-50), which satisfies the radiation condition at $x=\infty$, i.e. the one which corresponds to an outgoing wave. A fourth solution $R_3(x)$ exists, representing an incoming wave from infinity. $R_4(x)$ and $R_3(x)$ correspond to $\sqrt{x}\, H^{(2)}_{n+1/2}(x)$ and $\sqrt{x}\, H^{(1)}_{n+1/2}(x)$ of equation (1-47), respectively. Here v takes up only odd integral values v=n=1,3,5,... as will be seen (6 pp. 41-43).

For $R_3(x)$ and $R_4(x)$ we can obtain formal solutions by solving equation (1-50) around the singular point $x=\infty$. But the singularity is now irregular, of finite rank, in this case 1. According to well-established results in the theory of differential equations, the normal descending power series involved in the so obtained formal solutions $R_3(x)$ and $R_4(x)$ are asymptotic in the precise sense of Poincaré's definition (9 pp. 168-174 444-445, 10 pp. 69-72). They are good for numerical computations if x is large.

However, the biconical antenna involves the problem of matching the solutions across the boundary sphere S, figure (1-2). This requires, in turn, the evaluation of $R_1(x)$ and $R_4(x)$ at $x=\ell$, where ℓ is the electrical length of the antenna. In general, ℓ is small enough, unless the antenna is sufficiently long, and $R_{4(\ell)}$ can not be evaluated with the required accuracy by using the asymptotic series. On the other hand, if the antenna is long, $R_1(\ell)$ can not be evaluated accurately by using the convergent expressions for $R_1(x)$, since away from x=0, their convergence is slow. More generally, a convergent series is of no use for numerical calculations if we need values at points away from the center of their circle of convergence. The rate of convergence soon becomes slow as we move away from the center, even if we are

still away from the circumference of the convergence circle. The usefulness of a convergent series representation of a function is, in general, quite limited.

Since equation (1-50) is of the second order, any of its solutions can be expressed as a linear combination of two other independent solutions. That is, we have:

$$R_1(x) = A_{13}\, R_3(x) + A_{14}\, R_4(x) \qquad (1\text{-}52)$$

$$R_2(x) = A_{23}\, R_3(x) + A_{24}\, R_4(x)\ . \qquad (1\text{-}53)$$

Compare with the relations

$$J_{\nu+1/2}(x) = \tfrac{1}{2}\, H^{(2)}_{\nu+1/2}(x) + \tfrac{1}{2}\, H^{(1)}_{\nu+1/2}(x)$$

$$N_{\nu+1/2}(x) = \tfrac{i}{2}\, H^{(2)}_{\nu+1/2}(x) - \tfrac{i}{2}\, H^{(1)}_{\nu+1/2}(x)$$

corresponding to equation (1-47). If we can evaluate the coefficients of these linear relations, we answer all the problems arising. Equation (1-52) provides in essence an asymptotic representation for $R_1(x)$ and enables us to evaluate values of this function for large x. Also, solving (1-52) and (1-53) in terms of $R_4(x)$, we obtain:

$$R_4(x) = A_{41}\, R_1(x) + A_{42}\, R_2(x) \qquad (1\text{-}54)$$

an equation, which gives the analytic continuation of $R_4(x)$ in the vicinity of x=0 and enables us to evaluate its values for small x. The determination of the above coefficients is in itself a major problem. In effect, it constitutes the main problem of this investigation. This is precisely what we meant on page 1-3 when we referred to a "complete solution" of the problem. The present discussion also clarifies the statements made on pages 1-1, 1-2, 1-12, regarding the generality inherent in the biconical antenna.

It may be argued at this point that it is not actually necessary to extend the stratification beyond a certain value r_o or x_o. Beyond this point we can consider $\varphi(x)\equiv 1$ and, instead of $R_4(x)$, make use of $\sqrt{x}\, H^{(2)}_{n+1/2}(x)$ of equation (1-47). We assume, of course, that $\varphi(x_o)$ is very close to 1. This would introduce a new matching problem across the sphere $r=r_o$ or $x=x_o$, unless $x_o=\ell$, i.e. unless the stratification is terminated at the end of the antenna, an assumption which introduces a severe restriction into the problem, indeed reduces it to a very special case. An additional matching problem at $x=x_o$ would, of course, require additional computational work; but, more important, it is precisely the matching problem that introduces all the approximations to the solution of the, otherwise, exactly formulated problem of the biconical antenna. Apart from all these considerations, we would still need to evaluate $R_1(x)$ in the interval $0\leqq x\leqq x_o$ and also $R_2(x)$ in the interval $\ell\leqq x\leqq x_o$. Unless further severe limitations are introduced, the convergent series expressions for $R_1(x)$ and $R_2(x)$ will not be useful for values of x close to x_o and the necessity of obtaining the linear relations (1-52) and (1-53) would not be avoided. Not to mention the fact that specializations of this sort restrict the generality of the problem.

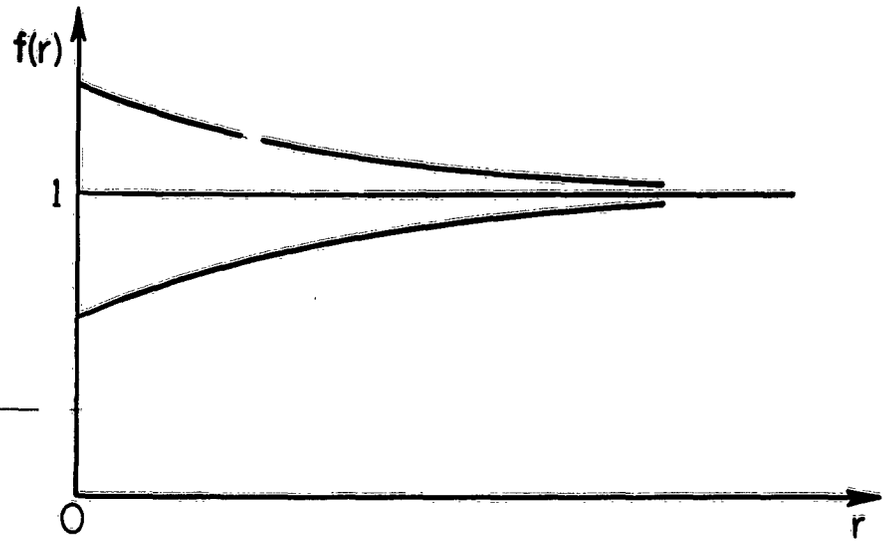

Fig. 1-1 General form of the "stratification function"

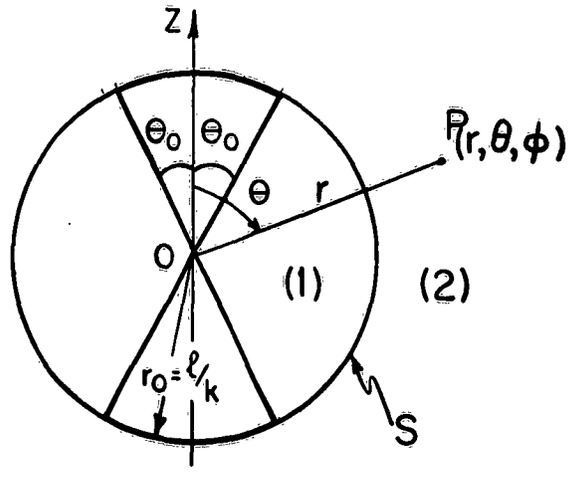

Fig. 1-2 Geometrical configuration

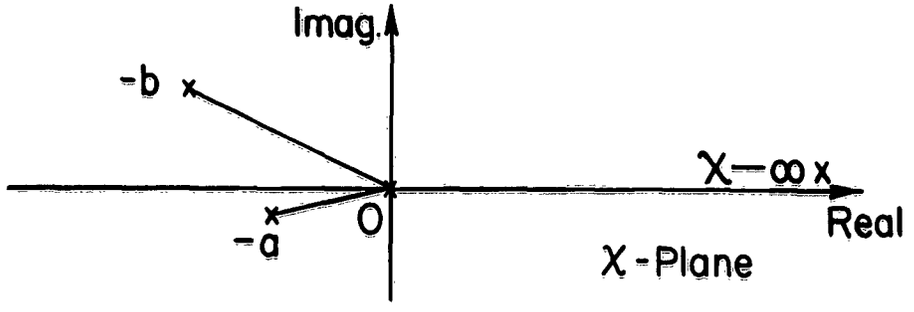

Fig. 1-3 Singularities of equation (1-50) in the χ-plane

CHAPTER 2

THE BICONICAL ANTENNA IMMERSED IN A RADIALLY STRATIFIED MEDIUM

The configuration is shown in figure (1-2). The results of the preceding chapter show that the biconical antenna theory for homogeneous media is readily applicable to stratified media if the proper solutions of the radial equations are used. We will not develop the theory step by step in this chapter. Detailed expositions can be found in references 5 and 6. We will make use of the results of the theory without deriving them, as long as it is obvious that they apply to the present case. Wherever essential modifications are necessary, the analysis will be given in detail.

In this connection the most important observation is that the angular equations for TM and TEM waves are not altered. It is then clear, that the problems of satisfying the boundary conditions and of matching the fields across the boundary S, at $x=\ell$, can be solved exactly as in the case of homogeneous media.

We start with the dominant, or TEM, interior mode. The field components were found in equations (1-37) and (1-39), or with $\kappa r=x$:

$$E_\theta(x,\theta) = -i\omega\mu\kappa \frac{R_o(x)}{x} \frac{1}{\sin\theta} \qquad (2\text{-}1)$$

$$H_\phi(x,\theta) = \frac{\kappa^2}{x} \frac{dR_o(x)}{dx} \frac{1}{\sin\theta} \quad , \qquad (2\text{-}2)$$

where $1/\sin\theta$ is the solution of the angular equation (1-35), the constant being included in $R_o(x)$. The equation for $R_o(x)$ is (1-44); with $\varphi(x)= \frac{x+a}{x+b}$ it becomes:

$$R_o''(x) + \frac{x+a}{x+b} R_o(x) = 0 \quad . \qquad (2\text{-}3)$$

Putting $x+b=z$ it becomes:

$$R_o''(z) + (1+c/z)\, R_o(z) = 0 \quad . \tag{2-4}$$

The solution of this equation can be expressed in terms of confluent hypergeometric functions. Put: $R_o(z) = ze^{\delta z}u(z)$. The equation for $u(z)$ is:

$$ze^{\delta z}u''(z)+2\frac{d}{dz}(ze^{\delta z})u'(z)+[(1+c/z)ze^{\delta z}+\frac{d^2}{dz^2}(ze^{\delta z})]u(z) = 0 \ ,$$

or, after division by $e^{\delta z}$:

$$zu''(z)+2(1+\delta z)u'(z)+[(1+\delta^2)z+c+2\delta]u(z) = 0 \quad .$$

Take $\delta=-1$ and change the independent variable $z=\beta t$:

$$\beta t\frac{u''(t)}{\beta^2}+(2-2i\beta t)\frac{u'(t)}{\beta}+(c-2i)u(t) = 0 \quad .$$

Finally put: $2i\beta=1$, $\beta=1/2i$, $z=t/2i$, $t=2iz$. The equation becomes:

$$tu''(t)+(2-t)u'(t)+(c/2i-1)u(t) = 0 \quad . \tag{2-5}$$

Comparing with the confluent hypergeometric equation:

$$xy''+(\gamma-x)y'-ay = 0 \ , \quad y = K_1F(a|\gamma|x)+K_2G(a|\gamma|x) \tag{2-6}$$

we see that a general solution of (2-5) is:

$$u(z) = K_1F(1+ic/2 \mid 2 \mid 2iz)+K_2G(1+ic/2 \mid 2 \mid 2iz) \tag{2-7}$$

Finally the general solution for $R_o(x)$ is:

$$R_o(x) = (x+b)e^{-ix}[K_1F(1+ic/2 \mid 2 \mid 2i(x+b))+ \\ +K_2G(1+ic/2 \mid 2 \mid 2i(x+b))] \ . \tag{2-8}$$

$G(a|\gamma|z)$ is the second solution of the confluent hyper-

geometric equation, the so-called Gordon function (11 pp. 577-646), when $\gamma = n = 1,2,3,\ldots$ is a positive integer. Here we have $\gamma = 2$.

Another set of independent solutions, the Whittaker functions, called $U_1(a|\gamma|z)$, $U_2(a|\gamma|z)$ in reference 11, are defined in terms of the following asymptotic series:

$$U_1(a|\gamma|z) \sim z^{a-\gamma}e^{z}\left[1+\frac{(1-a)(\gamma-a)}{z}+\ldots\ldots+\right. \tag{2-9}$$

$$\left.+\frac{(1-a)(2-a)\ldots(n-a)(\gamma-a)(\gamma-a+1)\ldots(\gamma-a+n-1)}{n!\,z^{n}}+\ldots.\right]$$

$$U_2(a|\gamma|z) \sim (-z)^{-a}\left[1-\frac{a(a-\gamma+1)}{z}+\ldots\ldots+\right. \tag{2-10}$$

$$\left.+(-1)^{n}\frac{a(a+1)\ldots(a+n-1)(a-\gamma+1)(a-\gamma+2)\ldots(a-\gamma+n)}{n!\,z^{n}}+\ldots\right]$$

where, with $z = |z|\,e^{i\phi}$ and $-\pi < \phi < \pi$, the following interpretation must be made:

$$-z = |z|\,e^{i(\phi-\pi)} \quad , \quad (-z)^{-a} = z^{-a}\,e^{i\pi a} \quad . \tag{2-11}$$

$R_o(x)$ can be expressed in terms of these solutions as follows:

$$R_o(x)=(x+b)e^{-ix}\left[K_3U_1(1+ic/2|2|2i(x+b))+\right.$$

$$\left.+K_4U_2(1+ic/2|2|2i(x+b))\right] \quad . \tag{2-12}$$

Numerical values for $F(1+ic/2|2|2i(x+b))$ and $G(1+ic/2|2|2i(x+b))$ are not tabulated. The argument is $z=2i(x+b)$ and in most cases, unless $|b|$ is very small, $|z|$ is large and renders the well-known convergent series expressions for these functions useless for numerical computations. It is more advantageous, therefore, to solve equation (2-3) directly around the non-singular point $x=0$. Such necessity does not arise, if $|b|$ is large enough to permit direct use of the asymptotic

expressions (2-9) and (2-10).

Equation (2-3) has a regular singularity at x=-b and a irregular one at x=∞. x=0 is an ordinary point. Convergent series expressions, valid for all values of x in the right half plane of interest and with a better rate of convergence, can be obtained, if we make the following change of variable:

$$t = \frac{x}{x+2b} \quad , \quad x = \frac{2bt}{1-t} \quad . \tag{2-13}$$

Bilinear transformations of this form will be used and discussed later, in Chapter 1, PART II, where the solution of (1-50) is investigated.

In terms of the new independent variable t equation (2-3) is expressed as follows:

$$(1-t)^3(1-t^2)\frac{d^2R_o(t)}{dt^2} - 2(1-t)^2(1-t^2)\frac{dR_o(t)}{dt} + \\ + 4b[(2b-a)t+a]R_o(t) = 0 \quad . \tag{2-14}$$

A regular singularity appears at t=-1, correspondingly to x=-b, an irregular at t=1, x=∞, while t=0, x=0, is an ordinary point. In order to obtain convergent series expansions around t=0 we put:

$$R_o(t) = \sum_{n=0}^{\infty} e_n t^n \quad , \quad |t|<1$$

and substitute into (2-14). Collecting coefficients of equal powers of t and equating to zero we obtain the recurrence formula for the coefficients:

$$e_n = \frac{1}{n(n-1)}\Big\{(n-1)(3n-4)e_{n-1} - 2[(n-2)(n-1)+2ba]e_{n-2} - [(n-3)(n-4) + \\ +2b(b-c)]e_{n-3} + (n-4)(3n-11)e_{n-4} - (n-4)(n-5)e_{n-5}\Big\} \quad ; \\ e_{-m} = 0 \quad , \quad m = 1,2,3,\ldots \quad . \tag{2-15}$$

The process leaves e_0 and e_1 undetermined as the constants of integration. Two independent solutions are defined as follows:

$$R_{o1}(x) = R_{o1}(t) = 1+e_2t^2+e_3t^3+\ldots \quad ; \; e_o = 1 \; , \; e_1 = 0 \; ; \; |t|<1 \qquad (2\text{-}16)$$

$$R_{o2}(x) = R_{o2}(t) = t+g_2t^2+g_3t^3+\ldots \quad ; \; g_o = 0 \; , \; g_1 = 1 \; ; \; |t|<1. \qquad (2\text{-}17)$$

The same recurrence formula (2-15) is used for both e_n's and g_n's, if the proper initial conditions, given in (2-16) and (2-17), respectively, are inserted. At x=0, t=0 we have:

$$R_{o1}(0)=1 \; , \; \left.\frac{dR_{o1}(x)}{dx}\right|_{x=0}=0 \; , \; R_{o2}(0)=0 \; , \; \left.\frac{dR_{o2}(x)}{dx}\right|_{x=0}=1/2b \; . \qquad (2\text{-}18)$$

In terms of these functions we can write:

$$R_o(x) = K_5 \, R_{o1}(x) + K_6 \, R_{o2}(x) \quad . \qquad (2\text{-}19)$$

Infinite Biconical Antenna: The field is expressed by equations (2-1),(2-2). The condition of an outgoing wave to infinity requires, in view of (2-9) and (2-10), that in the present case:

$$R_o(x) = C_o(x+b)e^{-ix}U_2(1+ic/2|2|2i(x+b)) \; , 0 \leqq \mathrm{Re}x \leqq \infty \; , \qquad (2\text{-}20)$$

where C_o is a constant. The transverse voltage and radial current in the upper cone are defined as follows:

$$V_o^{inf}(x) = \int_{\theta_o}^{\pi-\theta_o} E_\theta r d\theta = -\omega\mu R_o(x)\int_{\theta_o}^{\pi-\theta_o}\frac{d\theta}{\sin\theta} = -\omega\mu R_o(x)\,2\ln\cot\frac{\theta_o}{2} \qquad (2\text{-}21)$$

$$I_o^{inf}(x) = \left[\int_o^{2\pi} H_\phi r\sin\theta \, d\phi\right]_{\theta=\theta_o} = 2\pi\kappa R_o'(x) \quad . \qquad (2\text{-}22)$$

The so-called characteristic impedance of the biconical antenna is defined by:

$$Z_o = V_o^{inf}(x)/I_o^{inf}(x) = -\frac{i\omega\mu}{\pi\kappa}\frac{R_o(x)}{R_o'(x)}\ln\cot\frac{\theta_o}{2} \quad , \tag{2-23}$$

where $R_o(x)$ is defined in (2-20). For non-dissipative media it is real, because, despite the i factor, the functions $R_o(x)$ and $R_o'(x)$ are complex. But it is no longer a constant; it depends on the radial distance x. This is the most important effect caused by the stratification of the medium.

Finite Biconical Antenna of Electrical Length ℓ. Field Expressions: For the dominant TEM mode in the region $0 \leqq x \leqq \ell$ the field is given again by (2-1),(2-2). The solution $R_o(x)$ of the radial equation is given by either (2-12) or (2-19).

For the higher TM modes in all regions, the fields are given by (1-22) to (1-24). Introducing the electrical distance $x = \kappa r$ and remembering from (1-41), that in all cases we called: $\omega^2\mu\,\xi(r) = \kappa^2 f(r) = \kappa^2\varphi(x)$, where κ = constant, we can rewrite these equations as follows:

$$H_\phi(x,\theta) = \frac{R(x)}{x}\frac{dT}{d\theta} \tag{2-24}$$

$$E_\theta(x,\theta) = i\omega\mu\frac{R'(x)}{x\varphi(x)}\frac{dT}{d\theta} \tag{2-25}$$

$$E_r(x,\theta) = i\omega\mu\nu(\nu+1)\frac{R(x)}{x^2\varphi(x)}T(\theta) \quad . \tag{2-26}$$

For the interior TM modes in the region $0 \leqq x \leqq \ell$ we take $R(x) = R_1(x)$, where, as explained in Chapter 1, $R_1(x)$ is the solution of equation (1-50), which is finite at x=0. The precise definition of $R_1(x)$ is given in Chapter 1, PART II, by equation (1-10). T(θ) satisfies the Legendre differential equation (1-21). As in references 5 and 6 we choose the odd solution satisfying the symmetry condition about the ground plane $\theta=\pi/2$.

$$T(\theta) = M_\nu(\cos\theta) = \frac{1}{2}[P_\nu(\cos\theta) - P_\nu(-\cos\theta)] \quad . \tag{2-27}$$

We follow the notation of reference 6. In reference 5, the above function is denoted by $L_\nu(\cos\theta)$.

The boundary condition $E_r(x,\theta_o) = E_r(x,\pi-\theta_o) = 0$ yields the infinite set of characteristic values ν. It is expressed by the following transcendental equation:

$$M_\nu(\cos\theta_o) = 0 \quad . \tag{2-28}$$

For $0 \leqq x \leqq \ell$ the total interior field is then:

$$x^2 \varphi(x) E_{1r}(x,\theta) = \sum_\nu a_\nu \frac{R_{1\nu}(x)}{R_{1\nu}(\ell)} M_\nu(\cos\theta) \tag{2-29}$$

$$xE_{1\theta}(x,\theta) = \frac{1}{\varphi(x)} \sum_\nu \frac{a_\nu}{\nu(\nu+1)} \frac{R'_{1\nu}(x)}{R_{1\nu}(\ell)} \frac{d}{d\theta} M_\nu(\cos\theta) - i\omega\mu\kappa \frac{R_o(x)}{\sin\theta} \tag{2-30}$$

$$xH_{1\phi}(x,\theta) = \frac{\kappa}{i\omega\mu} \sum_\nu \frac{a_\nu}{\nu(\nu+1)} \frac{R_{1\nu}(x)}{R_{1\nu}(\ell)} \frac{d}{d\theta} M_\nu(\cos\theta) + \kappa^2 R'_o(x) \frac{1}{\sin\theta} \quad . \tag{2-31}$$

The subscript ν was added to $R_1(x)$ to denote the characteristic value to which it corresponds, while the added subscript 1 in E_{1r} etc., refers to the interior region (1) in figure (1-2). We must also remember, that the general solution $R(x)$ of (1-50) for $\nu=0$, can be expressed as $\kappa R'_o(x)$, where $R_o(x)$ is the general solution of (2-3) in either of the forms (2-12) or (2-19); with this in mind, we can check equations (2-29) to (2-31) dimensionally and prove them correct.

The total radial current in the upper cone is given by:

$$I(x) = \frac{2\pi}{\kappa} x \sin\theta_o H_{1\phi}(x,\theta_o) = I_o(x) + \bar{I}(x) \quad , \tag{2-32}$$

where:

$$I_o(x) = 2\pi\kappa R'_o(x) \tag{2-33}$$

is the principal current associated with the interior dominant TEM mode and

$$\bar{I}(x)= \frac{2\pi \sin\theta_o}{i\omega\mu} \sum_\nu \frac{a_\nu}{\nu(\nu+1)} \frac{\bar{R}_{1\nu}(x)}{\bar{R}_{1\nu(\ell)}} \frac{d}{d\theta} M_\nu(\cos\theta_o) \qquad (2\text{-}34)$$

is the complimentary current associated with the higher interior TM modes. From the definition (1-10), PART II, of $\bar{R}_{1\nu}(x)$ and for $\nu > 0$, we observe that $\bar{R}_{1\nu}(0) = 0$. Then:

$$\bar{I}(0) = 0 \quad , \quad I(0) = \bar{I}_o(0) \quad . \qquad (2\text{-}35)$$

The transverse voltage $\bar{V}(x)$ is defined by:

$$\bar{V}(x)= \int_{\theta_o}^{\pi-\theta_o} \frac{x}{\kappa} \bar{E}_{1\theta}\, d\theta = \frac{1}{\kappa}(-i\omega\mu\kappa)\bar{R}_o(x)\int_{\theta_o}^{\pi-\theta_o} \frac{d\theta}{\sin\theta} +$$

$$+ \frac{1}{\kappa\varphi(x)} \sum_\nu \frac{a_\nu}{\nu(\nu+1)} \frac{\bar{R}'_{1\nu}(x)}{\bar{R}_{1\nu(\ell)}} \int_{\theta_o}^{\pi-\theta_o} \frac{d}{d\theta} M_\nu(\cos\theta)\, d\theta \quad .$$

From (2-27), (2-28) we conclude that all the terms in the sum are 0. Thus:

$$\bar{V}(x) = \bar{V}_o(x) = -2i\omega\mu\bar{R}_o(x)\ln\cot\frac{\theta_o}{2} \qquad (2\text{-}36)$$

The so defined voltage is due only to the dominant mode, irrespectively of x. Calling:

$$\bar{z}_o= \frac{\omega\mu\ln\cot(\theta_o/2)}{\pi\kappa} \qquad (2\text{-}37)$$

and using (2-19) we can write:

$$I_o(x) = D_1 R'_{o1}(x) + D_2 R'_{o2}(x) \qquad (2\text{-}38)$$

$$i\,\frac{V(x)}{z_o} = D_1 R_{o1}(x) + D_2 R_{o2}(x) \quad . \qquad (2\text{-}39)$$

We will express D_1, D_2, $I_o(x)$, $V(x)$ in terms of $V(\ell)$ and the terminal admittance

$$Y_t = I_o(\ell)/V(\ell) \quad , \tag{2-40}$$

as seen by the dominant mode at $x=\ell$. At $x=\ell$ (2-38) and (2-39) yield:

$$D_1R_{o1}(\ell)+D_2R_{o2}(\ell)=iV(\ell)/\bar{z}_o \quad , \quad D_1R'_{o1}(\ell)+D_2R'_{o2}(\ell)=Y_tV(\ell) \ .$$

Then:

$$D_1 = \frac{V(\ell)}{\Delta}\begin{vmatrix} i/\bar{z}_o & R_{o2}(\ell) \\ Y_t & R'_{o2}(\ell) \end{vmatrix} \quad , \quad D_2 = \frac{V(\ell)}{\Delta}\begin{vmatrix} R_{o1}(\ell) & i/\bar{z}_o \\ R'_{o1}(\ell) & Y_t \end{vmatrix} \ ,$$

where $\Delta = \begin{vmatrix} R_{o1}(x) & R_{o2}(x) \\ R'_{o1}(x) & R'_{o2}(x) \end{vmatrix}$, the Wronskian of the particular solutions $R_{o1}(x)$, $R_{o2}(x)$ of equation (2-3), is a constant. Referring to (2-18) we find that:

$$\Delta = R_{o1}(x)\ R'_{o2}(x) - R'_{o1}(x)\ R_{o2}(x) = 1/2b \tag{2-41}$$

We may also use the definition (2-12), instead of (2-19), that is:

$$R_{o1}(x) = (x+b)e^{-ix}U_1(1+ic/2|2|2i(x+b))$$

$$R_{o2}(x) = (x+b)e^{-ix}U_2(1+ic/2|2|2i(x+b))$$

With the help of (2-9) to (2-11) and letting $x\to\infty$, we obtain:

$$R_{o1}(x) \xrightarrow[x\to\infty]{} -i2^{-1+ic/2}\ e^{-\pi c/4+2ib}\ x^{ic/2}\ e^{ix}$$

$$R'_{o1}(x) \xrightarrow[x\to\infty]{} 2^{-1+ic/2}\ e^{-\pi c/4+2ib}\ x^{ic/2}\ e^{ix}$$

$$R_{o2}(x) \xrightarrow[x\to\infty]{} i2^{-1-ic/2}\ e^{-\pi c/4}\ x^{-ic/2}\ e^{-ix}$$

$$R'_{o2}(x) \xrightarrow[x\to\infty]{} 2^{-1-ic/2}\, e^{-\pi c/4}\, x^{-ic/2}\, e^{-ix} \quad .$$

Then, in this case:

$$\Delta = -\frac{1}{2}\, e^{-\pi c/2+2ib} \quad . \tag{2-42}$$

Returning to (2-38),(2-39) we can write:

$$V(x) = \frac{V(\ell)}{\Delta}\,[(R'_{o2(\ell)}+i\bar{z}_o Y_t R_{o2(\ell)})R_{o1(x)} - (i\bar{z}_o Y_t R_{o1(\ell)}+R'_{o1(\ell)})R_{o2(x)}] \tag{2-43}$$

$$I_o(x) = \frac{V(\ell)}{\Delta}\,[(iR'_{o2(\ell)}/\bar{z}_o - Y_t R_{o2(\ell)})R'_{o1(x)} + (Y_t R_{o1(\ell)} - iR'_{o1(\ell)}/\bar{z}_o)R'_{o2(x)}] \quad . \tag{2-44}$$

The input admittance is defined by:

$$Y_i = \frac{I(0)}{V(0)} = \frac{I_o(0)}{V(0)} = \frac{1}{\bar{z}_o}\,\frac{[R'_{o2}(\ell)+i\bar{z}_o Y_t R_{o2}(\ell)]R'_{o1}(0) - [i\bar{z}_o Y_t R_{o1}(\ell)+R'_{o1}(\ell)]R'_{o2}(0)}{[R'_{o2}(\ell)+i\bar{z}_o Y_t R_{o2}(\ell)]R_{o1}(0) - [i\bar{z}_o Y_t R_{o1}(\ell)+R'_{o1}(\ell)]R_{o2}(0)} \quad . \tag{2-45}$$

and in this way it can be expressed in terms of Y_t only.

With the use of (2-33),(2-36),(2-37) we can rewrite the set (2-29) to (2-31) as follows:

$$x^2 \varphi(x) E_{1r}(x,\theta) = \sum_\nu a_\nu \frac{R_{1\nu}(x)}{R_{1\nu(\ell)}} M_\nu(\cos\theta) \tag{2-46}$$

$$xE_{1\theta}(x;\theta) = \frac{\omega\mu}{2\pi\bar{z}_o}\frac{V(x)}{\sin\theta} + \frac{1}{\varphi(x)}\sum_\nu \frac{a_\nu}{\nu(\nu+1)}\frac{R'_{1\nu}(x)}{R_{1\nu(\ell)}}\frac{d}{d\theta}M_\nu(\cos\theta) \tag{2-47}$$

$$xH_{1\phi}(x,\theta) = \frac{K}{2\pi}\frac{I_o(x)}{\sin\theta} + \frac{K}{i\omega\mu}\sum_\nu \frac{a_\nu}{\nu(\nu+1)}\frac{R_{1\nu}(x)}{R_{1\nu(\ell)}}\frac{d}{d\theta}M_\nu(\cos\theta) \quad . \tag{2-48}$$

In the region $\ell \leqq x \leqq \infty$ only higher TM modes appear. The field is expressed by equations (2-24) to (2-26). In order to satisfy the radiation condition we must now take $R(x)=R_4(x)$, where $R_4(x)$ was defined in Chapter 1; explicit expressions for this function will be given in Chapters 1 and 2, PART II. For the odd angular solution we must use:

$$T(\theta) = P_q(\cos\theta) \quad , \quad q = 1,3,5,\ldots . \tag{2-49}$$

Denoting $\sum_{q=1,3,5,\ldots}^{\infty} \equiv \sum_q'$ we can express the total exterior field in the region $\ell \leqq x \leqq \infty$ as follows:

$$x^2 \varphi(x) E_{2r}(x,\theta) = \sum_q' b_q \frac{R_{4q}(x)}{R_{4q}(\ell)} P_q(\cos\theta) \tag{2-50}$$

$$xE_{2\theta}(x,\theta) = \frac{1}{\varphi(x)} \sum_q' \frac{b_q}{q(q+1)} \frac{R_{4q}'(x)}{R_{4q}(\ell)} \frac{d}{d\theta} P_q(\cos\theta) \tag{2-51}$$

$$xH_{2\phi}(x,\theta) = \frac{\kappa}{i\omega\mu} \sum_q' \frac{b_q}{q(q+1)} \frac{R_{4q}(x)}{R_{4q}(\ell)} \frac{d}{d\theta} P_q(\cos\theta) \quad . \tag{2-52}$$

Matching of the Fields. Input Admittance: The continuity and boundary conditions across the spherical surface at $x=\ell$, can be expressed as follows:

$$E_{2r}(\ell,\theta) = E_{1r}(\ell,\theta) \quad , \quad \theta_o < \theta < \pi-\theta_o \tag{2-53}$$

$$\begin{aligned} E_{2\theta}(\ell,\theta) &= E_{1\theta}(\ell,\theta) \quad , \quad \theta_o < \theta < \pi-\theta_o \\ &= 0 \quad , \quad 0 \leqq \theta \leqq \theta_o \text{ and } \pi-\theta_o \leqq \theta \leqq \pi \end{aligned} \tag{2-54}$$

$$H_{2\phi}(\ell,\theta) = H_{1\phi}(\ell,\theta) \quad , \quad \theta_o < \theta < \pi-\theta_o \tag{2-55}$$

We will first obtain an expression for the terminal admittance Y_t. Equation (2-45) will then provide an expression for the input admittance Y_1. At $x=\ell$ we obtain from (2-48):

$$\ell H_\phi = \frac{K}{2\pi}\frac{Y_t V(\ell)}{\sin\theta} + \frac{K}{i\omega\mu}\sum_\nu \frac{a_\nu}{\nu(\nu+1)}\frac{d}{d\theta}M_\nu(\cos\theta) \quad .$$

Integrating from $\theta=\theta_o$ to $\theta=\pi-\theta_o$ we observe that, by virtue of (2-27),(2-28), the terms corresponding to the summation $\sum_\nu$ vanish. Therefore:

$$\int_{\theta_o}^{\pi-\theta_o} \ell H_\phi(\ell,\theta)d\theta = \frac{KY_tV(\ell)}{2\pi}\int_{\theta_o}^{\pi-\theta_o}\frac{d\theta}{\sin\theta} = \frac{KY_tV(\ell)}{\pi}\ln\cot\frac{\theta_o}{2} =$$

$$= \frac{K^2 Z_o}{\omega\mu}V(\ell)Y_t$$

Integrating $xH_\phi(\ell,\theta)$ the same way, but using now its expression in (2-52) and equating we finally obtain:

$$Y_t = \frac{2i}{KZ_oV(\ell)}\sum_q{}' \frac{b_q}{q(q+1)}P_q(\cos\theta_o) \quad . \qquad (2\text{-}56)$$

The coefficients b_q will all turn out to be proportional to $V(\ell)$. So, $V(\ell)$ cancels in the above expression for Y_t.

The remaining step is the matching problem. We write the sets of equations (2-46)-(2-48) and (2-50)-(2-52) for $x=\ell$ and substitute into (2-55). It suffices to match only the electric field, or, alternatively, the components H_ϕ and E_θ. The procedure is based upon the orthogonal properties of the Legendre functions and is fully explained in references 5 and 6. Since the stratification does not affect the angular functions the matching problem follows lines identical with the case of homogeneous media. There result two infinite systems of linear algebraic equations relating the sets of coefficients a_ν and b_q. The coefficients themselves are determined by solving these linear systems of equations. In the present case the only difference from the homogeneous problem appears in the coefficients of equations (2-46)-(2-48) and (2-50)-(2-52), when written for $x=\ell$. We will not, therefore, repeat the process of matching. It follows the method explained in full in references 5 and 6. The results in the present case

are as follows:

$$a_\nu = \sum_q{}' u_{\nu q} b_q \tag{2-57}$$

$$b_q = -\frac{\omega\mu(2q+1)}{2\pi z_o Z_q^+} V(\ell) P_q(\cos\theta_o) + \sum_\nu \frac{Z_\nu^-}{Z_q^+} v_{q\nu} \quad , \tag{2-58}$$

where:

$$u_{\nu q} = \frac{2\nu+1}{q(q+1)-\nu(\nu+1)} P_q(\cos\theta_o) / \left[\frac{\partial M_\nu(\cos\theta_o)}{\partial \nu}\right] \tag{2-59}$$

$$v_{q\nu} = \frac{q(q+1)}{\nu(\nu+1)} \frac{2q+1}{\nu(\nu+1)-q(q+1)} \sin\theta_o P_q(\cos\theta_o) \frac{dM_\nu(\cos\theta_o)}{d\theta_o} \tag{2-60}$$

$$Z_q^+ = \frac{1}{Y_q^+} = \frac{1}{\varphi(\ell)} \frac{R'_{4q}(\ell)}{R_{4q}(\ell)} = \frac{\ell+b}{\ell+a} \frac{R'_{4q}(\ell)}{R_{4q}(\ell)} \tag{2-61}$$

$$Z_\nu^- = \frac{1}{Y_\nu^-} = \frac{1}{\varphi(\ell)} \frac{R'_{1\nu}(\ell)}{R_{1\nu}(\ell)} = \frac{\ell+b}{\ell+a} \frac{R'_{1\nu}(\ell)}{R_{1\nu}(\ell)} \quad . \tag{2-62}$$

Substituting the a_ν's from (2-57) into (2-58) we can obtain the following infinite linear set of equations containing only the coefficients b_q:

$$b_q = -\frac{\omega\mu(2q+1)}{2\pi z_o Z_q^+} V(\ell) P_q(\cos\theta_o) + \sum_\nu \frac{Z_\nu^-}{Z_q^+} v_{q\nu} \sum_m{}' u_{\nu m} b_m \quad . \tag{2-63}$$

This shows more clearly that all b_q's (and, consequently, all a_ν's) turn out to be proportional to $V(\ell)$.

From this point on all the approximations for the solution of (2-57) and (2-58), or (2-63), in special cases, like small-angle cones, large-angle cones etc., follow lines identical with the case of homogeneous media, as explained in references 5 and 6.

Small-Angle Biconical Antennas: In the limiting case of θ_o approaching zero, the system of equations (2-63) can be solved (5 pp. 833-834, 12, 13). The method of solution, applicable in the present case, is identical with the one used in reference 5. The following limiting values hold as $\theta_o \to 0$:

$$\nu \doteq k+1/\ln(2/\theta_o) = k+\delta \quad , \quad \delta = 1/\ln(2/\theta_o) \quad , \quad k = 1,3,5,\ldots \tag{2-64}$$

$$\frac{dM_\nu(\cos\theta_o)/d\theta_o}{\partial M_\nu(\cos\theta_o)/\partial\nu} = -\frac{d\nu}{d\theta_o} \doteq -\frac{1}{\theta_o[\ln(2/\theta_o)]^2} = -\frac{(\nu-k)^2}{\theta_o} = -\frac{\delta^2}{\theta_o} \tag{2-65}$$

$$P_q(\cos\theta_o) \doteq 1 \quad . \tag{2-66}$$

Calling:

$$B_q = -\frac{2\pi\bar{Z}_o}{\varpi\mu V_{(\ell)}} b_q \tag{2-67}$$

and making use of the above relations, we can write equations (2-63) as follows:

$$\frac{Z_q^+}{2q+1} B_q + q(q+1) \sum_k{}' \sum_m{}' \frac{B_m}{Y_{k+\delta}^-} \Psi(k,m,q) \doteq 1 \tag{2-68}$$

$$\Psi(k,m,q) = \frac{(2k+1+2\delta)\delta^2}{(k+\delta)(k+\delta+1)(k+\delta-q)(k+\delta+q+1)(m-k-\delta)(m+k+\delta+1)} \quad . \tag{2-69}$$

In the limit $\theta_o \to 0$, $\delta \to 0$ we have:

$$\begin{aligned}
\Psi(k,m,q) &\sim \delta^2 \doteq 0 && \text{if } k \neq q \ , \ m \neq k \\
&\sim \delta \doteq 0 && \text{if } k \neq q \ , \ m = k \\
&\sim \delta \doteq 0 && \text{if } k = q \ , \ m \neq k \\
&\doteq -\frac{1}{q(q+1)(2q+1)} && \text{if } k = q = m \quad .
\end{aligned}$$

Only the last case, k=q=m, contributes significantly to the sums in (2-68), which, in the limit, can be simplified to:

$$\frac{Z_q^+}{2q+1} B_q - q(q+1) B_q Z_{q+\delta}^- / [q(q+1)(2q+1)] \doteq 1 \quad .$$

Thus:

$$B_q \doteq \frac{2q+1}{Z_q^+ - Z_{q+\delta}^-} \doteq \frac{2q+1}{Z_q^+ - Z_q^-} \qquad (2\text{-}70)$$

So, in the limit of small-angle cones:

$$Y_t \doteq -\frac{i\omega\mu}{\pi\kappa z_o^2} \sum_q{}' \frac{2q+1}{q(q+1)} \frac{1}{Z_q^+ - Z_q^-} \quad . \qquad (2\text{-}71)$$

It is interesting to examine how Y_t and Y_i behave as ℓ, the electrical length of the antenna, approaches zero. This short-antenna limit will serve as a check and explanation of the numerical results obtained in the next chapter, in this particular case. Using (2-61) and (2-62) we can write:

$$Z_q^+ - Z_q^- = \frac{\ell+b}{\ell+a} \left[R'_{4q}(\ell)/R_{4q}(\ell) - R'_{1q}(\ell)/R_{1q}(\ell) \right]$$

As $\ell \to 0$, the behaviour of $R_{iq}(\ell)$ and $R_{2q}(\ell)$ can be found from the results of Chapters 1 and 2, PART II. We refer, first, to equation (1-54):

$$R_{4q}(\ell) \equiv A_{41} R_{1q}(\ell) + A_{42} R_{2q}(\ell) \quad .$$

On the other hand, series expressions for $R_{1q}(\ell)$ and $R_{2q}(\ell)$ can be written down at once, by merely inspecting equation (1-50):

$$R_{1q}(\ell) = \ell^{q+1}(1+a_1\ell+\dots\dots)$$

$$R_{2q}(\ell) = R_{1q}(\ell)\ln\ell + \frac{b_o+b_1\ell+\dots}{\ell^q} \quad , \; b_o \neq 0 \; , \; q = \text{integer} \; .$$

In Chapter 1, PART II, these series are developed in full, but, for our present purpose, we can do without any reference to the results of this chapter. Thus, as $\ell \to 0$:

$$\frac{R'_{1q}(\ell)}{R_{1q}(\ell)} = \frac{q+1}{\ell} + \frac{a_1+2a_2\ell+\dots}{1+a_1\ell+\dots} \doteq \frac{q+1}{\ell} \qquad (2\text{-}72)$$

$$\frac{R_{2q}(\ell)}{R_{1q}(\ell)} = \ln\ell + \frac{1}{\ell^{2q+1}} \frac{b_o+b_1\ell+\dots}{1+a_1\ell+\dots} \doteq \frac{b_o}{\ell^{2q+1}} \tag{2-73}$$

$$\frac{R'_{2q}(\ell)}{R_{1q}(\ell)} = \frac{1}{\ell} + \frac{R'_{1q}(\ell)}{R_{1q}(\ell)} \ln\ell + \frac{b_1+2b_2\ell+\dots}{2q+1(1+a_1\ell+\dots)} -$$

$$- \frac{q}{\ell^{2q+2}} \frac{b_o+b_1\ell+\dots}{1+a_1\ell+\dots} \doteq - \frac{b_o q}{\ell^{2q+2}} \tag{2-74}$$

$$\frac{R'_{4q}(\ell)}{R_{4q}(\ell)} = \frac{[R'_{1q}(\ell)/R_{1q}(\ell)]+(A_{42}/A_{41})[R'_{2q}(\ell)/R_{1q}(\ell)]}{1 + (A_{42}/A_{41})[R_{2q}(\ell)/R_{1q}(\ell)]} \pm$$

$$\pm \frac{(q+1)/\ell - (A_{42}/A_{41})(b_o q/\ell^{2q+2})}{1 + (A_{42}/A_{41})(b_o/\ell^{2q+1})} \doteq - \frac{q}{\ell} \tag{2-75}$$

$$Z_q^+ - Z_q^- \doteq - \frac{b}{a} \frac{2q+1}{\ell}$$

Substituting in (2-71) we obtain:

$$Y_t \doteq \ln 2 \frac{i\omega\mu}{\pi\kappa\bar{z}_o^2} \frac{a}{b} \ell \quad . \tag{2-76}$$

In the above equation use of the identity $\sum_q' \frac{1}{q(q+1)} = \ln 2$ was made. Therefore, as $\ell \to 0$, $Y_t \to 0$.

The input impedance is given by (2-45), which, with the use of (2-18), reduces to:

$$Z_1 = 2bi\bar{z}_o \frac{R'_{o2}(\ell)+i\bar{z}_o Y_t R_{o2}(\ell)}{R'_{o1}(\ell)+i\bar{z}_o Y_t R_{o1}(\ell)} \quad . \tag{2-77}$$

Using (2-13) together with (2-16) and (2-17) we find:

$$R_{o1}(\ell) = 1+e_2 \frac{\ell^2}{(\ell+2b)^2} + O(\ell^3) = 1+ \frac{e_2}{4b^2}\ell^2+O(\ell^3) \tag{2-78}$$

$$R'_{o1}(\ell) = \frac{e_2}{2b^2}\ell + O(\ell^2) = -\frac{a}{b}\ell + O(\ell^2) \qquad (2\text{-}79)$$

$$R_{o2}(\ell) = \frac{\ell}{2b} + O(\ell^2) \qquad (2\text{-}80)$$

$$R'_{o2}(\ell) = \frac{1}{2b} + O(\ell) \quad . \qquad (2\text{-}81)$$

Substituting into (2-77) and letting $\ell \to 0$, we obtain:

$$Z_1 \doteq -\frac{b}{a}\frac{i\bar{Z}_o + O(\ell)}{[1+\frac{\omega\mu}{\pi\kappa\bar{Z}_o}\ln 2]\ell + O(\ell^2)} \doteq -\frac{b}{a}\frac{i\bar{Z}_o}{1+\frac{\ln 2}{\ln\cot\theta_o/2}}\frac{1}{\ell} \quad . \qquad (2\text{-}82)$$

We observe that, as $\ell \to 0$, $Z_1 \to \infty$ as $1/\ell$. For a non-dissipative medium a, b, $\bar{Z}_o$ and ℓ are all real and Z_1 is large and capacitive. For a dissipative medium a, b, $\ell = \kappa r_o$, $\bar{Z}_o$ are complex and both R_1 and X_1 go to infinity.

Wide-Angle Biconical Antennas: In the case of homogeneous media, it is well known that a good approximation to Y_t can be obtained, if we neglect the higher order internal TM waves (6 pp. 41-43, 13, 15). For stratified media, however, it can be anticipated that such an approximation will not be as good, since, with the assumed variation $f(x) = (x+a)/(x+b)$, the stratification function changes more rapidly for small x, i.e., inside the antenna in region (1), figure (1-2), f(x) varies more rapidly than outside. It is natural to assume, that more internal waves will be needed in this region to account for this greater variation. One is left with no other alternative but to solve the infinite set of equations (2-57) and (2-58). It is still very instructive, however, to obtain a solution in the following two cases: when only the principal TEM mode is retained, all the internal TM modes being neglected, and, secondly, when, in addition to the principal TEM mode, the first TM internal mode is retained and all the higher neglected. In both cases, the set

of equations (2-57) and (2-58) can be solved explicitly for the coefficients b_q. In the case of homogeneous media, the difference between Y_{to} and Y_{t1}, the zeroth and first order approximations obtained in this manner, is practically very small (6 pp. 41-43, 13), justifying the assumption whereby all higher internal modes were neglected. For stratified media, as the results of Chapter 3 show, $Y_{to} - Y_{t1}$ is small for relatively long antennas, roughly one wavelength and longer. For such lengths the assumption that the internal TM waves are unimportant and can be neglected is still valid. For shorter antennas, however, in the same medium, $Y_{to} - Y_{t1}$ and, as a result, $Z_{io} - Z_{i1}$ are large, in agreement with the prediction mentioned above. One should then retain more internal waves and solve the system of equations for the b_q's separately for each assumed length ℓ in this range of values.

In the zeroth order approximation neglecting all internal TM modes, i.e. assuming that all $a_v = 0$, we immediately obtain from (2-58):

$$b_q = - \frac{\omega\mu(2q+1)}{2\pi \bar{z}_o Z_q^+} V(\ell) P_q(\cos\theta_o) \quad . \tag{2-83}$$

Substitution into (2-56) yields:

$$Y_{to} = - \frac{i\omega\mu}{\pi\kappa \bar{z}_o^2} \sum_q{}' \frac{2q+1}{q(q+1)} Y_q^+ P_q^2(\cos\theta_o) \quad . \tag{2-84}$$

For the first order approximation we retain the first internal TM mode, in addition to the principal TEM mode, and neglect all the others. In other words we assume:

$$a_{v1} = \sum_q{}' u_{v1q} b_q \quad , \quad a_{v2} = a_{v3} = \ldots = 0 \quad . \tag{2-85}$$

From equation (2-58) we obtain in this case:

$$b_q = - \frac{\omega\mu(2q+1)}{2\pi} Y_q^+ V(\ell) P_q(\cos\theta_o) + \frac{Y_q^+}{Y_{v1}^-} v_{qv1} \sum_q{}' u_{v1q} b_q \quad . \tag{2-86}$$

It is convenient at this point to introduce a change in the notation to make the formulas comparable to C. T. Tai's results in the homogeneous case (13, 6 pp. 41-43). We call:

$$I_{vq} = \int_{\theta_o}^{\pi-\theta_o} M_v(\cos\theta) P_q(\cos\theta) \sin\theta \, d\theta \qquad (2\text{-}87)$$

$$N_v = \int_{\theta_o}^{\pi-\theta_o} [M_v(\cos\theta)]^2 \sin\theta \, d\theta \quad . \qquad (2\text{-}88)$$

Then, from (2-59),(2-60) and Schelkunoff's formulas (6 pp. 47-48), we have:

$$u_{vq} = I_{vq}/N_v \quad , \quad v_{qv} = -\frac{(2q+1)q(q+1)}{2v(v+1)} I_{vq} \quad . \qquad (2\text{-}89)$$

Equations (2-86) can now be written as follows:

$$b_q = -\frac{\omega\mu(2q+1)}{2\pi} Y_q^+ V(\ell) P_q(\cos\theta_o) - \frac{Y_q^+}{Y_{v1}^-} \frac{(2q+1)q(q+1)}{2v_1(v_1+1)} \frac{I_{v1q}}{N_{v1}} A_{v1} \qquad (2\text{-}90)$$

$$A_{v1} = \sum_q{}' I_{v1q} b_q \quad . \qquad (2\text{-}91)$$

Multiply (2-90) by I_{v1q} and sum over q = 1,3,5,... . With the use of (2-91) we obtain:

$$A_{v1} = -\frac{\omega\mu}{2\pi z_o} V(\ell) \sum_q{}' (2q+1) Y_q^+ P_q(\cos\theta_o) I_{v1q} -$$

$$- \frac{A_{v1}}{Y_{v1}^- N_{v1} 2v_1(v_1+1)} \sum_q{}' (2q+1)q(q+1) Y_q^+ I_{v1q}^2 \quad ,$$

or:

$$A_{v1} = -\frac{(\omega\mu/2\pi z_o) V(\ell) \sum_q{}' (2q+1) Y_q^+ P_q(\cos\theta_o) I_{v1q}}{1 + \dfrac{\sum_q{}' (2q+1)q(q+1) Y_q^+ I_{v1q}}{Y_{v1}^- N_{v1} 2v_1(v_1+1)}}$$

Substituting back into (2-90) we find:

$$b_q = -\frac{\omega\mu}{2\pi\bar{z}_o} V(\ell)\left[(2q+1)Y_q^+ P_q(\cos\theta_o) - Y_q^+(2q+1)q(q+1)I_{v1q} \cdot \right.$$
$$\left. \cdot \frac{\sum_q'(2q+1)Y_q^+ P_q(\cos\theta_o) I_{v1q}}{2v_1(v_1+1)N_{v1}Y_{v1}^- + \sum_q'(2q+1)q(q+1)Y_q^+ I_{v1q}^2}\right] . \qquad (2\text{-}92)$$

Finally from (2-56) we obtain:

$$Y_{t1} = Y_{to}^+ + \frac{i\omega\mu}{\pi\kappa\bar{z}_o^2} \frac{\left[\sum_q'(2q+1)Y_q^+ P_q(\cos\theta_o) I_{v1q}\right]^2}{2v_1(v_1+1)N_{v1}Y_{v1}^- + \sum_q'(2q+1)q(q+1)Y_q^+ I_{v1q}^2} . \qquad (2\text{-}93)$$

This equation is in agreement with the result of C. T. Tai (6 pp. 41-43, 13) obtained, for homogeneous media, by application of a variational principle.

For the short antenna limit, letting $\ell \to 0$, we find from (2-61) and (2-75):

$$Y_q^+ \doteq -\frac{a}{b}\frac{\ell}{q} . \qquad (2\text{-}94)$$

Then from (2-84):

$$Y_{to} \doteq \frac{i\omega\mu}{\pi\kappa\bar{z}_o^2}\frac{a}{b}\left[\sum_q'\frac{2q+1}{q^2(q+1)}P_q^2(\cos\theta_o)\right]\ell . \qquad (2\text{-}95)$$

Thus, after comparing with (2-76), in the limit $\ell \to 0$ Y_t and, consequently, Z_i for wide-angle antennas behave in a way similar to thin antennas, as explained in the preceding subsection.

CHAPTER 3

NUMERICAL COMPUTATIONS

INTRODUCTION

Numerical results were obtained with the use of an IBM 7090 computer. Six distinct cases of stratified media were considered, heretofore numbered I to VI, and in each case the cone angle θ_o, figure (1-2), was given 8 different values:

$\theta_o = 1/20^\circ,\ 1/4^\circ,\ 1^\circ,\ 2^\circ,$ for the small-angle case,

$\theta_o = 30^\circ,\ 39.23^\circ,\ 55^\circ,\ 70^\circ,$ for the wide-angle case.

The special value $\theta_o = 39.23^\circ$ in the latter case was chosen, because it yields an integral value for the first characteristic root of equation (2-28), namely:

$$\nu_1 = 3 \ , \tag{3-1}$$

facilitating the evaluation of Y_{t1} and Z_{i1} (13).

In each case the input impedance $Z_i = R_i + iX_i$ of the antenna in Ohms was computed and plotted as a function of the physical length of the antenna r_o. For thin antennas, the terminal admittance Y_t is independent of the cone angle θ_o, according to equation (2-71). We call:

$$YT = GT+iST = \bar{z}_o^2 Y_t = -\frac{i\omega\mu}{\pi\kappa} \sum_q{}' \frac{2q+1}{q(q+1)} \frac{1}{Z_q^+ - Z_q^-} \ . \tag{3-2}$$

This characteristic quantity for thin antennas was also plotted in Ohms versus r_o in each case, figure (3-2).

<u>Case I:</u> In view of the fact that no experimental data are

available concerning the behaviour of a biconical antenna in a radially stratified medium and in order to check the theory, we considered in Case I a non-dissipative medium slightly stratified so that, at a certain frequency, the stratification function has the following form:

$$\varphi(x) = \frac{x+12}{x+10} \quad , \quad a = 12 \quad , \quad b = 10 \tag{3-3}$$

$$x = \kappa r = \omega\sqrt{\mu\epsilon_o}\, r \quad , \quad \kappa = \omega\sqrt{\mu\epsilon_o} \quad , \quad \ell = \kappa r_o \tag{3-4}$$

$$\frac{\epsilon(r)}{\epsilon_o} = f(r) = \frac{r+12/\kappa}{r+10/\kappa} \quad . \tag{3-5}$$

Thus, at the origin $\epsilon(0) = 1.2\epsilon_o$, while for large r the dielectric constant reduces to ϵ_o, the free-space value. $Z_1=R_1+iX_1$ and, for thin cones, $Y\bar{T}=G\bar{T}+iS\bar{T}$, in Ohms, were plotted in figures (3-3),(3-4) and (3-2), respectively, versus $\ell = \omega\sqrt{\mu\epsilon_o}\, r_o$. It is natural to anticipate that these curves will be close to known results (5 p. 837, 15) for homogeneous media with $\epsilon=\epsilon_o$ and $\epsilon = 1.2\epsilon_o$, thus providing a check on the theory. The prediction is completely justified as will be seen in the next section.

Cases II to V: In all these cases the antenna is immersed in a stratified and dissipative medium similar to the conducting solution used in Iizuka's experiments with linear antennas (14). The complex dielectric factor is:

$$\xi(r) = \epsilon(r)[1-iT(r)] \quad , \tag{3-6}$$

where $T=\tan\delta=\sigma/\omega\epsilon$, the loss tangent, can vary from 0.036 to 8.8, while ϵ/ϵ_o changes correspondinly from 78 to 69 (14 p. 3). In these ranges such variations can be represented very closely by the following functional dependences:

$$\epsilon(r) = \epsilon_o\epsilon_f \frac{r+d}{r+d\epsilon_f/78} \tag{3-7}$$

$$\bar{T}(r) = T_f \frac{r+d0.036/T_f}{r+d} \quad . \tag{3-8}$$

Thus, at r=0: $\epsilon(0)=78\epsilon_o$, $\bar{T}(0)=0.036$, while for large r, $\epsilon(r)\to\epsilon_f\epsilon_o$ and $\bar{T}(r)\to T_f$. The parameters ϵ_f and T_f control the final values of $\epsilon(r)$ and $\bar{T}(r)$, their ranges being:

$$78 \geqslant \epsilon_f \geqslant 69 \quad , \quad 0.036 \leqslant T_f \leqslant 8.8 \quad , \tag{3-9}$$

while d affects their slope. There is a correspondence between values of ϵ and $\bar{T}=\sigma/\omega\epsilon$, which, for the conducting solution under consideration, has been determined experimentally and plotted (14 opp. p. 7). It is a simple matter to see if the assumed variations (3-7) and (3-8) agree with this curve. Even in the extreme case $\epsilon_f=69$ and $T_f=8.8$, one obtains:

$$\epsilon(r) = \epsilon_o 69 \frac{r/d+1}{r/d+69/78} \quad , \quad \bar{T}(r) = 8.8 \frac{r/d+0.036/8.8}{r/d+1} \quad .$$

Elimination of r/d between these two equations yields:

$$\frac{\epsilon(r)}{\epsilon_o} = 69/\left[1+\frac{3(\bar{T}(r)-8.8)}{26\times 8.764}\right] \quad , \tag{3-10}$$

a relation, which, in the above ranges (3-9), agrees closely with the experimental curve mentioned above. For intermediate values of ϵ_f and T_f the ranges of $\epsilon(r)$ and $\bar{T}(r)$ are smaller, i.e.

$$78 \geqslant \epsilon(r)/\epsilon_o \geqslant \epsilon_f \quad , \quad 0.036 \leqslant \bar{T}(r) \leqslant T_f \tag{3-11}$$

and the correspondence between $\epsilon(r)$ and $\bar{T}(r)$ is correct, as long as ϵ_f and T_f themselves satisfy (3-10). So, ϵ_f and T_f are not independent parameters, but are related according to equation (3-10).

The assumed variations (3-7) and (3-8), in addition to satisfying the above requirements, lead to a stratification function $\varphi(x)$ in the form (1-48). Substituting (3-7),(3-8) into

(3-6), we obtain:

$$\omega^2\mu\,\xi(r) = \omega^2\mu\epsilon_o\epsilon_f(1-iT_f)\,\frac{r+d(1-10.036)/(1-iT_f)}{r+d\epsilon_f/78} \quad . \qquad (3\text{-}12)$$

Calling:

$$K = \omega\sqrt{\mu\epsilon_o\epsilon_f} \qquad (3\text{-}13)$$

$$\bar{K} = K\sqrt{1-iT_f} \qquad (3\text{-}14)$$

$$x = \bar{K}r \quad , \quad \bar{\ell} = \bar{K}r_o \qquad (3\text{-}15)$$

we can write (3-12) as follows:

$$\omega^2\mu\,\xi(r) = \bar{K}^2\,\frac{x+S(1-10.036)/\sqrt{1-iT_f}}{x+S(\epsilon_f/78)\sqrt{1-iT_f}} = \bar{K}^2\,\varphi(x) = \bar{K}^2\,\frac{x+a}{x+b} \quad , \qquad (3\text{-}16)$$

where:

$$a = S(1-10.036)/\sqrt{1-iT_f} \qquad (3\text{-}17)$$

$$b = S(\epsilon_f/78)\sqrt{1-iT_f} \qquad (3\text{-}18)$$

$$S = Kd = \omega\sqrt{\mu\epsilon_o\epsilon_f}\,d \quad . \qquad (3\text{-}19)$$

We can also write (3-7) and (3-8) as follows:

$$\frac{\epsilon(r)}{\epsilon_o} = \epsilon_f\,\frac{Kr+S}{Kr+S(\epsilon_f/78)} \quad , \quad T(r) = T_f\,\frac{Kr+S(0.036/T_f)}{Kr+S} \quad . \qquad (3\text{-}20)$$

Two independent parameters appear: T_f, controlling the final value of the loss tangent of the medium, and S, controlling the slope of the stratification function. ϵ_f is found from T_f with the use of (3-10). Different values of these parameters correspond to different media. Note, also, that S depends on frequency. The independent variable is the physical length of the antenna r_o. Introducing electrical units and referring to the common initial values, we use as independent variable the following quantity:

$$\ell = \omega\sqrt{\mu\epsilon_o 78}\, r_o = \kappa\sqrt{78/\epsilon_f}\, r_o \quad . \tag{3-21}$$

Note that x varies in the fourth quadrant of the complex x-plane from 0 to ∞ along the straight line connecting the origin and the point x=b.

Cases II to V refer to different stratified media with the following values of the independent parameters:

$$\text{Case II}: \quad T_f = 1\,, \quad S = 8\,, \quad \epsilon_f = 76.897 \tag{3-22}$$

$$\text{Case III}: \quad T_f = 1\,, \quad S = 6\,, \quad \epsilon_f = 76.897 \tag{3-23}$$

$$\text{Case IV}: \quad T_f = 1\,, \quad S = 4\,, \quad \epsilon_f = 76.897 \tag{3-24}$$

$$\text{Case V}: \quad T_f = 2\,, \quad S = 6\,, \quad \epsilon_f = 75.785 \quad . \tag{3-25}$$

Cases II, III, IV can also be considered as referring to the same stratified medium, but correspondig to different frequencies. $\epsilon(r)/\epsilon_o$ and T(r) for all 4 cases, as given by equation (3-20), are plotted in figure (3-1), versus $y = \omega\sqrt{\mu\epsilon_o 78}\, r = \sqrt{78/\epsilon_f}\,\kappa r$.

Case VI: In contrast to the previous cases, where the conductivity of the medium increases away from the center of the antenna, Case VI refers to a medium in which T(r) starts, at r=0, from a high value T_i and decreases to 0.036 as $r \to \infty$, while $\epsilon(r)/\epsilon_o$ starting from ϵ_i increases to 78 as $r \to \infty$.

$$\epsilon(r) = \epsilon_o 78\, \frac{r+d}{r+d78/\epsilon_i} \tag{3-26}$$

$$T(r) = 0.036\, \frac{r+dT_i/0.036}{r+d} \quad . \tag{3-27}$$

It can easily be checked that the requirement of correspondence between $\epsilon(r)$ and T(r) is satisfied in the ranges:

$$69 \leqslant \epsilon_i \leqslant \epsilon(r)/\epsilon_o \leqslant 78 \quad , \qquad 8.8 \geqslant T_i \geqslant T(r) \geqslant 0.036 \quad , \tag{3-28}$$

as long as ϵ_i and T_i satisfy (3-10).

In place of (3-12) to (3-20) we have now:

$$\omega^2\mu\,\xi(r) = \omega^2\mu\epsilon_0 78(1-i0.036)\,\frac{r+d(1-iT_1)/(1-i0.036)}{r+d(78/\epsilon_1)} \qquad (3\text{-}29)$$

$$\kappa = \omega\sqrt{\mu\epsilon_0 78} \qquad (3\text{-}30)$$

$$\bar{\kappa} = \kappa\sqrt{1-i0.036} \qquad (3\text{-}31)$$

$$x = \bar{\kappa}r \quad , \quad \bar{\ell} = \bar{\kappa}r_0 \qquad (3\text{-}32)$$

$$\omega^2\mu\,\xi(r) = \bar{\kappa}^2\varphi(x) = \bar{\kappa}^2\,\frac{x+a}{x+b} \qquad (3\text{-}33)$$

$$a = S(1-iT_1)/\sqrt{1-i0.036} \qquad (3\text{-}34)$$

$$b = S(78/\epsilon_1)\sqrt{1-i0.036} \qquad (3\text{-}35)$$

$$S = \kappa d = \omega\sqrt{\mu\epsilon_0 78}\,d \qquad (3\text{-}36)$$

$$\frac{\epsilon(r)}{\epsilon_0} = 78\,\frac{\kappa r+S}{\kappa r+S(78/\epsilon_1)} \quad , \quad T(r) = 0.036\,\frac{\kappa r+S(T_1/0.036)}{\kappa r+S} \qquad (3\text{-}37)$$

As independent variable the same quantity:

$$\ell = \omega\sqrt{\mu\epsilon_0 78}\,r_0 = \kappa r_0 \qquad (3\text{-}38)$$

was chosen. The following values were given to the parameters:

$$\text{Case VI :} \quad T_1 = 1 \,, \quad S = 6 \,, \quad \epsilon_1 = 76.897 \qquad (3\text{-}39)$$

$\epsilon(r)/\epsilon_0$ and $T(r)$, as given by (3-37), are also plotted in figure (3-1), versus the same variable $y = \omega\sqrt{\mu\epsilon_0 78} = \kappa r$.

In Cases II to VI equation (2-37) defining $\bar{z}_0$ must be written as follows:

$$\bar{z}_0 = [\omega\mu\ln\cot(\theta_0/2)]/\pi\bar{\kappa} \quad . \qquad (3\text{-}40)$$

For all Cases II to VI and in terms of the same independent variable $\ell = \omega\sqrt{\mu\epsilon_0 78}\,r_0$:

$YT = Z_o^2 Y_t = GT+iST$, for thin cones, in Ohms, is plotted in figure (3-2). The input impedance $Z_i = R_i+iX_i$, in Ohms, is plotted in figures (3-5),(3-6),(3-7),(3-8), for $\theta_o = 1/20^o$, $1/4^o$, 1^o, 2^o, respectively. For wide-angle cones, the zeroth order approximation $Z_{io} = R_{io}+iX_{io}$, in Ohms, is plotted in figures (3-9),(3-10),(3-11), for $\theta_o = 30^o$, 55^o, 70^o, respectively. Finally, for $\theta_o = 39.23^o$, the zeroth and first order approximations Z_{io} and Z_{i1}, in Ohms, are plotted in figures (3-12),(3-13),(3-14),(3-15) and (3-16), for Cases II, III, IV, V, VI, respectively.

DISCUSSION OF THE RESULTS AND CONCLUSIONS

All computations were performed with single, 8-decimal, precision. By far, the major problem was the evaluation of $R_1(x)$, $R_2(x)$, $R_3(x)$, $R_4(x)$ and their derivatives, as well as the coefficients of the asymptotic expansions (1-52),(1-53). Remarks relative to the computation of these quantities will be postponed until, in Chapters 1 and 2, PART II, the defining formulas are developed. As a general observation, we note that the smoother the stratification function, the closer the singularities $x=-a$ and $x=-b$ of equation (1-50) are spaced; this, in turn, makes the overlapping region between the convergent and asymptotic series expressions for $R_1(x)$ or $R_2(x)$, wider and the agreement better. In Case I, for instance, in the middle of the overlapping region, agreement of 4 significant decimals was obtained for the lower order functions. As the stratification function becomes sharper, the overlapping region narrows and the agreement worsens. This was observed in Cases IV and V, characterized by a sharper $\varphi(x)$; in a region falling roughly between $\ell = 3.4$ and $\ell = 4.2$, for thin cones, the plotted points deviated slightly from a smooth line, in contrast to all other regions and cases where the smoothness of the curves was remarkable. No attempt was made to obtain more accurate values

in this short region in Cases IV and V, since the deviations were small and the use of an improved series would alter the computer program.

For wide-angle cones, the situation is less critical in this respect, as far as R_{1o}, X_{1o} and R_{11}, X_{11} are concerned, for reasons similar to the homogeneous case (12, 13). Furthermore, in equation (2-71) for thin cones, $Z_q^+ - Z_q^- = \frac{\bar{\ell}+b}{\bar{\ell}+a}[R_{4q}(\bar{\ell})/R_{4q}(\bar{\ell}) - R_{1q}(\bar{\ell})/R_{1q}(\bar{\ell})]$ appears. In contrast, only $Z_q^+ = \frac{\bar{\ell}+b}{\bar{\ell}+a}[R_{4q}(\bar{\ell})/R_{4q}(\bar{\ell})]$ appears in Y_{to} and Y_{t1}, equations (2-84) and (2-93), for wide-angle cones. In dissipative media, $R_{3q}(\bar{\ell})$ and $R_{4q}(\bar{\ell})$ are no longer complex conjugates of each other and the asymptotic series for $R_{4q}(\bar{\ell})$ always starts working earlier, i.e. for smaller $|\bar{\ell}|$, than the asymptotic series for $R_{3q}(\bar{\ell})$. The separating region becomes wider as the dissipation increases. At the same time, the convergent series for $R_{1q}(\bar{\ell})$ converges faster and works farther than the convergent series for $R_{2q}(\bar{\ell})$. Therefore, the evaluation of $R_{1q}(\bar{\ell})$ and Z_q^- through

$$R_{1q}(\bar{\ell}) = A_{13}R_{3q}(\bar{\ell}) + A_{14}R_{4q}(\bar{\ell}),$$

as well as the evaluation of $R_{4q}(\bar{\ell})$ and Z_q^+ through

$$R_{4q}(\bar{\ell}) = A_{41}R_{1q}(\bar{\ell}) + A_{42}R_{2q}(\bar{\ell}) ,$$

become critical in the intermediate region, making the evaluation of Y_t less accurate for thin cones. The former difficulty is also the reason for not extending the curves for thin cones as far as for wide-angle cones, especially in Cases IV and V; the series for $R_3(\bar{\ell})$ can not be used yet. These remarks do not apply in the real case. $R_{4q}(\ell)$ and $R_{3q}(\ell)$ are complex conjugates of each other, as will be seen in Chapter 1, PART II. Thus, $R_3(\ell)$ is not actually involved.

If the variations of $\varphi(x)$ are still sharper, no overlapping region may exist. If one is interested in lengths ℓ falling in the region where neither the convergent series work, nor the asymptotic are valid, one should try to develop better convergent series (such possibilities exist as will be seen in Chapter 1, PART II), or else use either analytic continuation or numerical integration of the differential equation. The author prefers analytic continuation to numerical integration.

The overlapping region between convergent and asymptotic expressions of the functions narrows and the accuracy in this region worsens as the order v or q of the functions increases. The same is true regarding the accuracy with which the coefficients A_{41}, A_{42} etc., of the asymptotic expansions (1-52) and (1-53) are evaluated. Fortunately, as the order increases, the effect of the higher-order modes on the final results diminishes and the restrictions of accuracy can be relaxed progressively.

The preceding remarks show that the accuracy of R_i and X_i is not the same for all values of ℓ in a given case. It may also differ from thin to wide-angle cones in the same medium. The variation in accuracy increases the sharper the stratification function becomes.

Case I was chosen to check the theory by comparison with available results in the homogeneous case (5 p. 837, 15). Comparing with the results plotted in figures (3-3) and (3-4), we observe a remarkable agreement. For $\theta_o = 1^o$ and 2^o, the "peculiar" behaviour of R_i at the second and third maximum and of X_i near $\ell = 9$ is reproduced here in almost identical form (5 p. 837). The same is true about the behaviour of R_{io} and X_{io} around their maxima for $\theta_o = 55^o$ and 70^o (15). In case I, 20 higher order terms were retained, i.e. terms up to and including q = 39 were kept. The accuracy for R_i and X_i is of the order of 0.1% , even better for small ℓ. In the impedance transformation from Y_t to Z_i, through equation (2-45), both expressions (2-12) and (2-19)

for $R_o(x)$ were used, yielding identical results. The former, in terms of the asymptotic series (2-9) and (2-10), worked very well in Case I. In all other Cases II to VI, (2-19), together with (2-16) and (2-17), worked better and was used.

For $\theta_o = 39.23^o$, the difference between Z_{io} and Z_{i1}, as seen in figure (3-4), is very small for $\ell \geqslant 4$. Thus, for wide-angle cones, Z_{io} is a good approximation to Z_i for such lengths. However, for $\ell < 4$ the difference is large, becoming larger as ℓ decreases, in contrast to the homogeneous case where this difference is small up to $\ell = 0$ (6 pp. 41-43, 13, 15). The reason for this disagreement was explained in the last subsection of the preceding chapter. One must keep more internal TM modes when $\ell < 4$ and solve the system of equations (2-57),(2-58) separately for each ℓ. This holds for $\theta_o = 30^o$, 55^o, 70^o and all values of θ_o in this range. Z_{io}, as plotted in figure (3-4), is only a rough approximation to Z_i for $\ell < 4$. The same must be said about Z_{i1}, since values of Z_{i2} or Z_{i3} are not available for comparison.

The number of higher modes retained in Cases II to VI was restricted by the accuracy, with which the coefficients A_{14}, A_{13} etc., of the asymptotic expansions (1-52),(1-53) could be evaluated. With an 8-decimal machine precision, beyond a certain q_{max} (which decreases as the stratification becomes sharper), it was not possible to evaluate these coefficients with any reasonable accuracy. This restriction was mentioned previously. It did not prove to be a serious problem in the cases investigated in this research. For sharper stratifications one can use double precision arithmetic, if it proves necessary. Beyond a certain ℓ, the asymptotic series for $R_4(\bar{\ell})$ can be used for the direct evaluation of $Z_q^+ = 1/Y_q^+ = \frac{\bar{\ell}+b}{\ell+a}\left[R'_{4q}(\bar{\ell})/R_{4q}(\bar{\ell})\right]$. For wide-angle cones, that is all that is necessary for the evaluation of Y_{to} and Y_{t1}, according to (2-84) and (2-93). It was observed that for such ℓ, in general, Z_{io} or Z_{i1} were good approximations to Z_i.

Since the coefficients A_{14}, A_{13} etc., are not involved any more, the number of terms retained can be increased at will to yield the required accuracy for such ℓ. In Cases II to V, 20 terms, up to and including q=39, were retained in this region.

We give below q_{max}, the order of the highest mode retained for thin cones and wide-angle cones of short length.

Case II : q_{max}= 33

Case III: q_{max}= 27

Case IV : q_{max}= 21

Case V : q_{max}= 23

Case VI : q_{max}= 31 .

Note how q_{max} drops in Cases IV and V, characterized by a sharper stratification. The accuracy of the final results is better than 1% in Cases II, III, VI, about 1% in Cases IV and V. It improves for small ℓ and, for wide-angle cones, beyond a certain ℓ, after which it was possible to retain more modes, as explained previously. For thin cones, in Cases IV and V, the accuracy becomes worse than 1% in the region extending roughly between ℓ=3.4 and ℓ=4.2 for reasons explained previously. Beyond ℓ=4.2 it improves, as the asymptotic series for $R_4(\ell)$ becomes more accurate.

In general, as far as the accuracy of the final results is concerned, the number of modes retained is not as critical as the accuracy with which the functions are evaluated. In Case I, even with 15 higher modes retained, no considerable change occured in the final results.

The difference $Z_{1o} - Z_{11}$ for θ_o=39.23°, figures (3-12) to (3-16), is small beyond ℓ=4, but large for $\ell < 4$ for all Cases II to VI. The same remarks as given for Case I, apply to these cases as well.

The behaviour of R_1 as $\ell \to 0$, is in conformity with the approximate formulas (2-82) and (2-95). With no dissipation,

Case I, $R_i \to 0$ as $\ell \to 0$. In dissipative media, Cases II to VI, it goes to infinity and at a faster rate as the dissipation increases.

Concerning the more important effects of dissipation, we observe the following: The oscillations of R_i and X_i versus ℓ are not displaced. The maxima and minima occur at almost the same values of ℓ, quite independently of the profile of the stratification. Even in Cases II, IV and VI, for example, characterized by quite different $\varphi(x)$, the displacements of resonance and antiresonance in Z_i are negligible. Thus, even in stratified media, the electrical length of the antenna is an important characteristic quantity, determining its properties in a manner quite independent of the medium.

However, the oscillations are dumped as the dissipation increases and R_i and X_i become almost constant beyond a certain value of ℓ. The effect is more pronounced and occurs at shorter lengths for higher dissipations as well as for larger θ_o. These effects have been observed experimentally in dissipative media (14). By increasing the length of the antenna, we do not affect the input current, hence Z_i, because the current leaks into the medium along the length of the antenna and quickly becomes negligible away from the center. Beyond this point, additional antenna length does not affect the current distribution.

For similar reasons, in stratified media the value of the dissipation in the immediate vicinity of the antenna plays a decisive role on its properties, the value of σ away from the center having practically no effect. Such effects have been observed experimentally (14). They can be seen very clearly here, comparing Case VI with the rest. Looking at figure (3-1), we see that medium VI is less dissipative, overall, than the media in Cases IV or V, for instance. However, $T(r)$ starts, at $r=0$, from a higher value in medium VI than in media IV and V. In the immediate vicinity of the antenna, medium VI is more dissipative than medium IV or V. The above-mentioned effects of dissipation

are much more pronounced in Case VI than in any other case.

Another result in agreement with experiment (14), concerns the final, almost constant, value of X_i for large ℓ. X_i is inductive in this region, its value getting larger as the dissipation increases. Compare Case VI, especially, with the rest.

The preceding observations show that, in dissipative media, no additional useful information is gained by extending the computations beyond the value of ℓ, after which Z_i becomes practically constant. Difficulties in evaluating $R_1(\bar{\ell})$, $R_2(\bar{\ell})$ and $R_3(\bar{\ell})$ for large $|\bar{\ell}|$, mentioned previously, are avoided. For higher dissipations, the value of ℓ, up to which the computations must be carried, decreases.

As a final remark, we observe that the whole analysis is based on the assumption that the stratification function f(r) can be approximated by a certain functional dependence. In the light of the results obtained, this assumption is justified. Cases II, III and IV refer to media for which f(r) differs from case to case, but not much and keeps the same general form, figure (3-1). $f^{III}_{(r)}$ varies in-between $f^{II}_{(r)}$ and $f^{IV}_{(r)}$. So does Z^{III}_i, varying in all cases and for all ℓ in-between Z^{II}_i and Z^{IV}_i and quite close to them, figures (3-3) to (3-11). The same behaviour is observed in Case I, if the comparison is made with homogeneous media for which $\epsilon/\epsilon_o = 1$ and $\epsilon/\epsilon_o = 1.2$. $f^{I}_{(r)}$ can be considered as an approximation to these homogeneous media. One can also state that, in a dissipative and stratified medium, the approximation of the actual variation by the assumed f(r) must be better for small r (i.e. in the immediate vicinity of the antenna) than for large r. Even large discrepancies, occuring away from the center, will not affect the results.

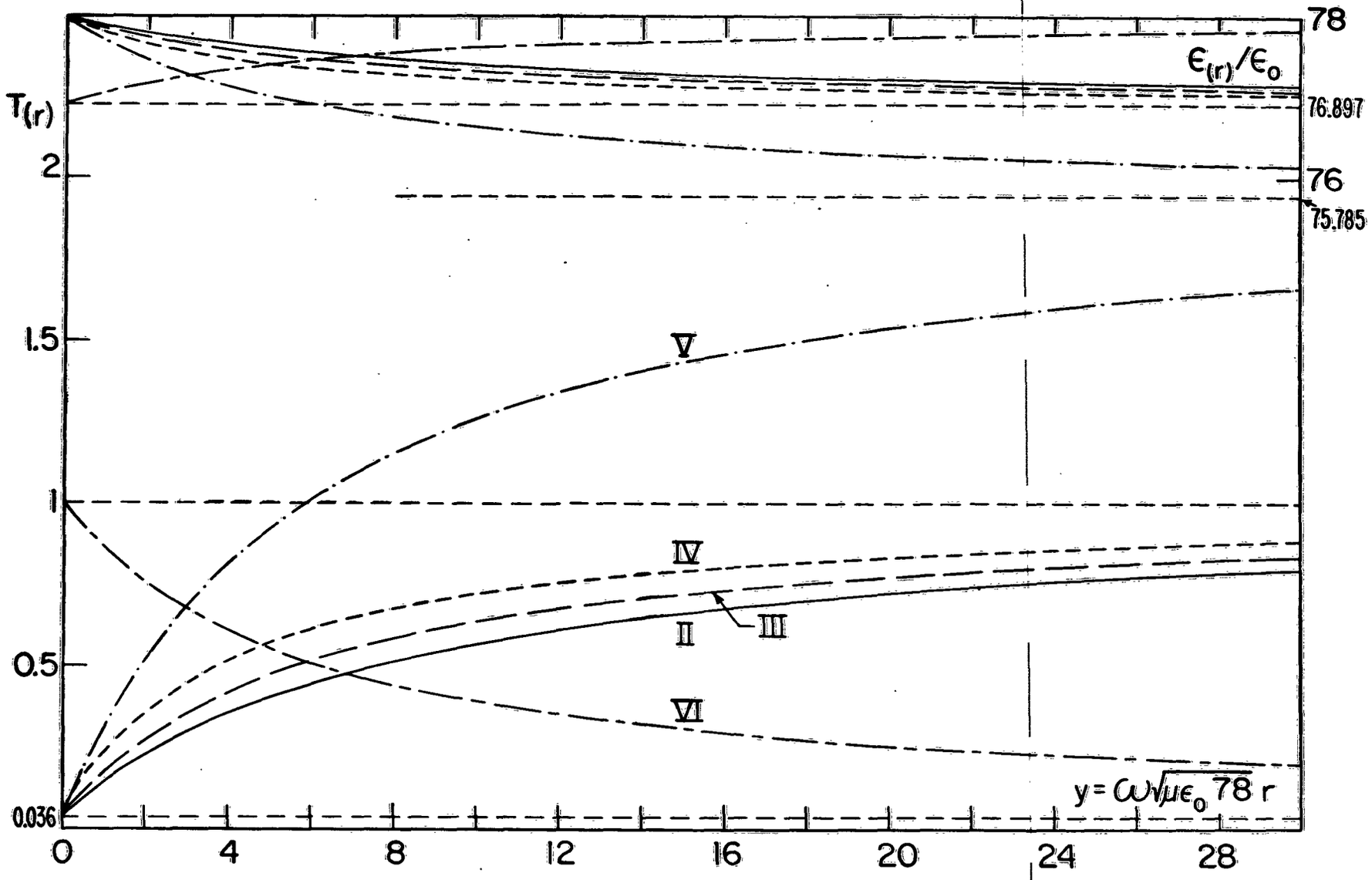

FIG. 3-1 VARIATIONS OF $T_{(r)}$ (LEFT SCALE) AND $\epsilon_{(r)}/\epsilon_0$ (RIGHT SCALE) VS. $y = \omega\sqrt{\mu\epsilon_0\,78}\,r$ IN MEDIA II TO VI.

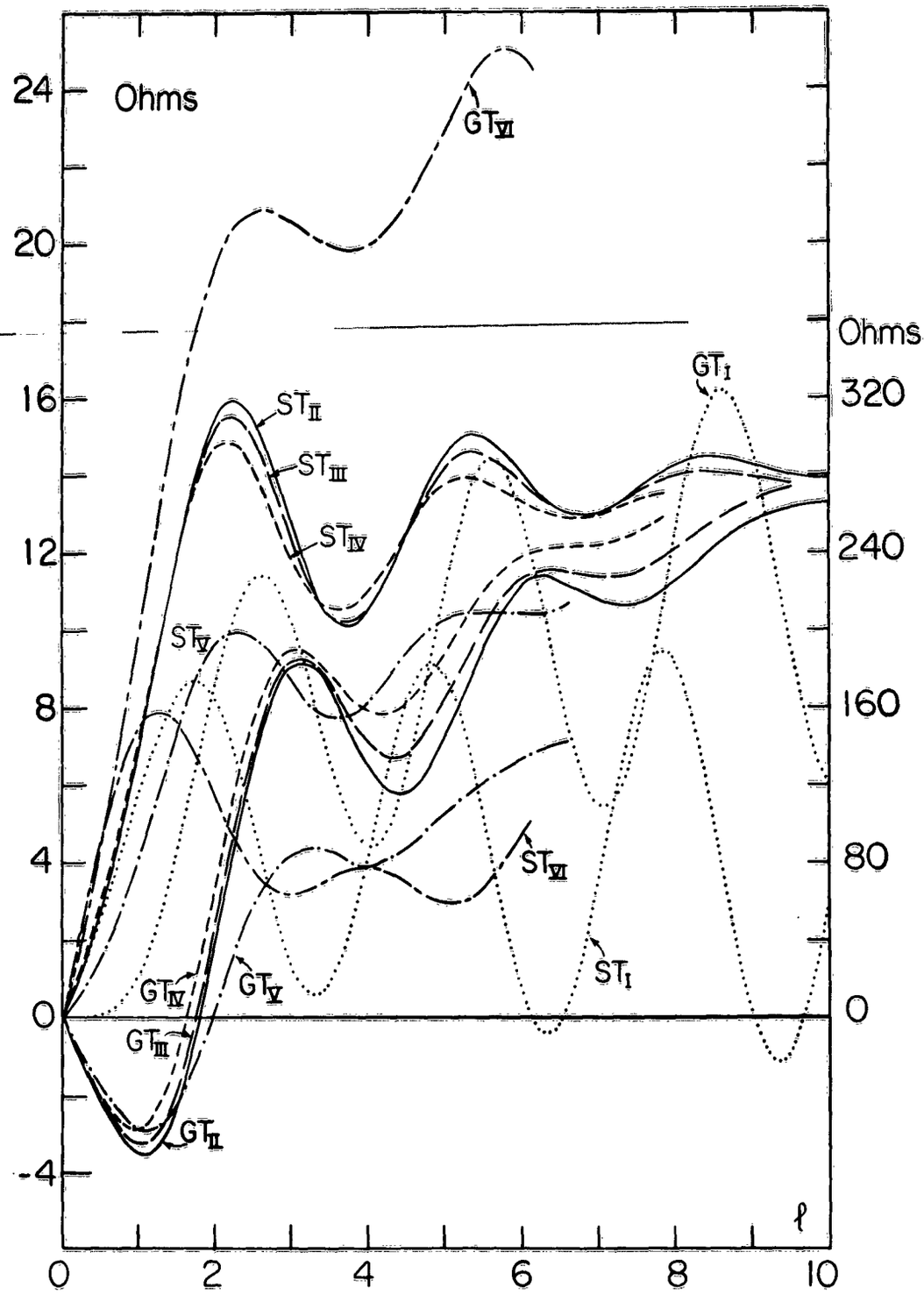

FIG. 3-2 THIN ANTENNAS $YT = \bar{Z}_0^2\, Y_t = GT + iST$, IN OHMS VS. ℓ. MEDIUM I: RIGHT SCALE, $\ell = \omega\sqrt{\mu\epsilon_0}\, r_0$ MEDIA II TO VI: LEFT SCALE, $\ell = \omega\sqrt{\mu\epsilon_0 78}\, r_0$.

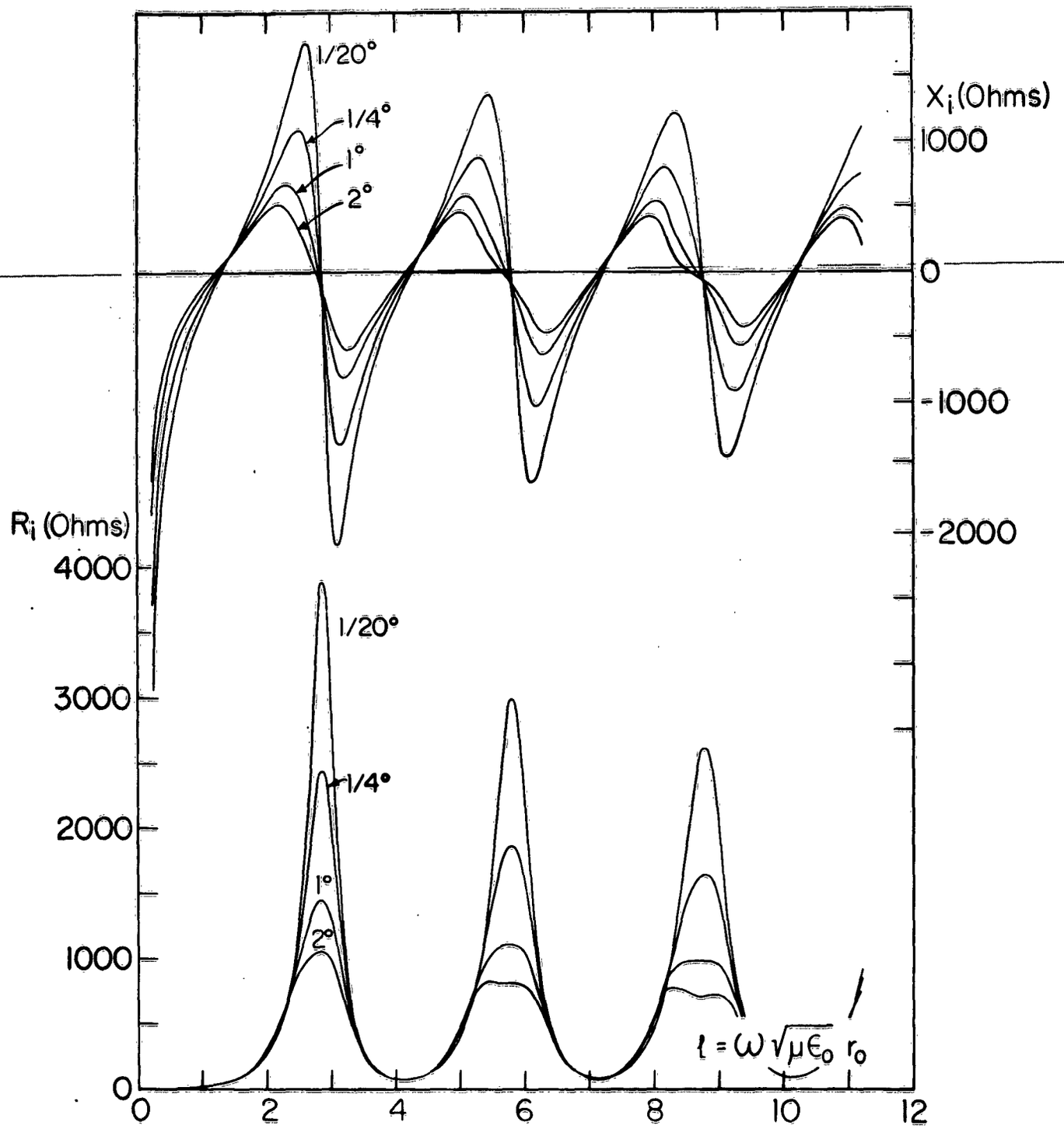

FIG. 3-3 THIN ANTENNAS. $Z_i = R_i + iX_i$ IN OHMS VS. ℓ IN MEDIUM I. R_i : LEFT SCALE; X_i : RIGHT SCALE

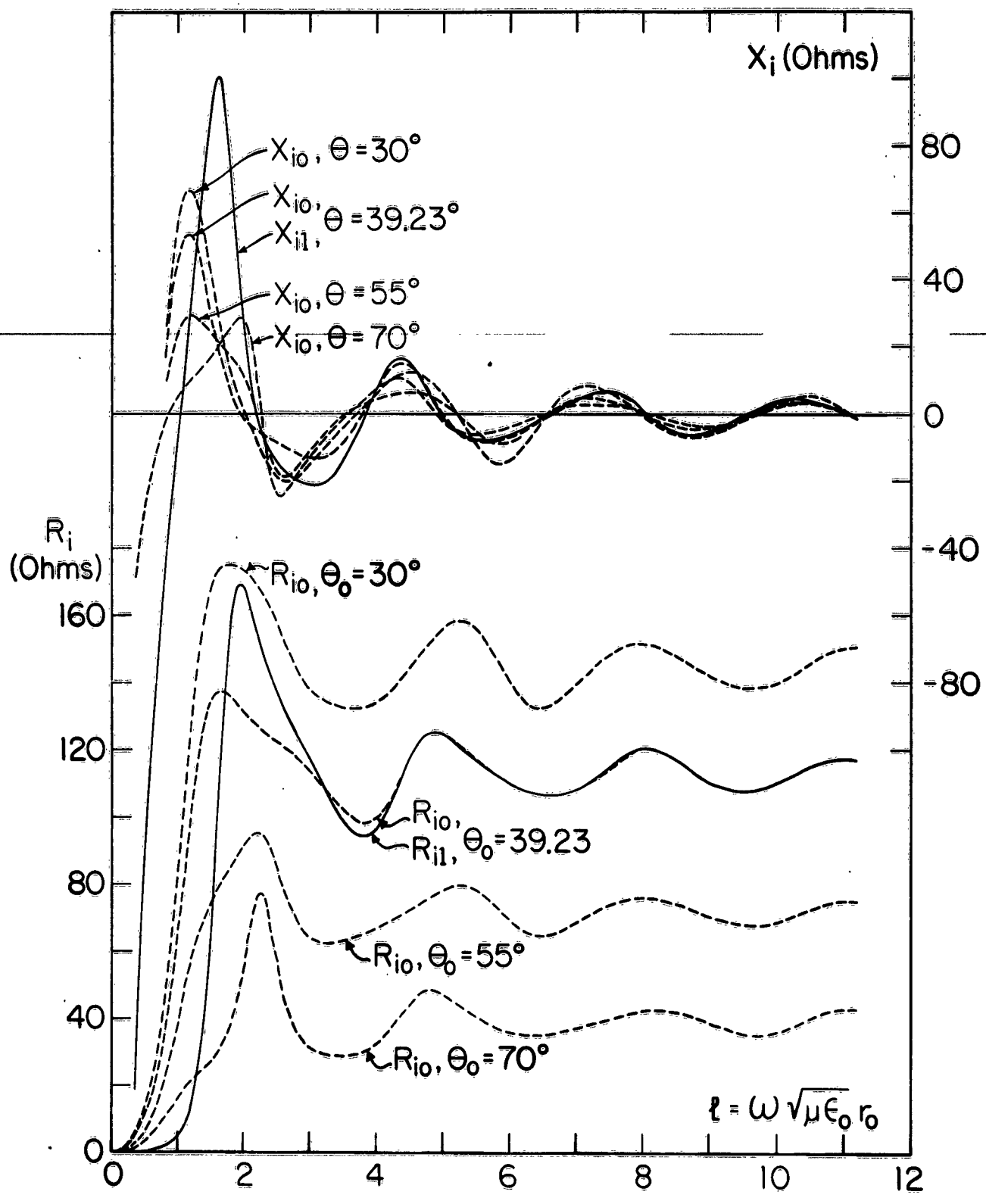

FIG. 3-4 MEDIUM I, WIDE-ANGLE ANTENNAS. $Z_{io} = R_{io} + iX_{io}$ IN OHMS VS. ℓ, *DOTTED LINE*. $Z_{il} = R_{il} + iX_{il}$ FOR $\Theta_0 = 39.23°$. R_i : LEFT SCALE; X_i : RIGHT SCALE

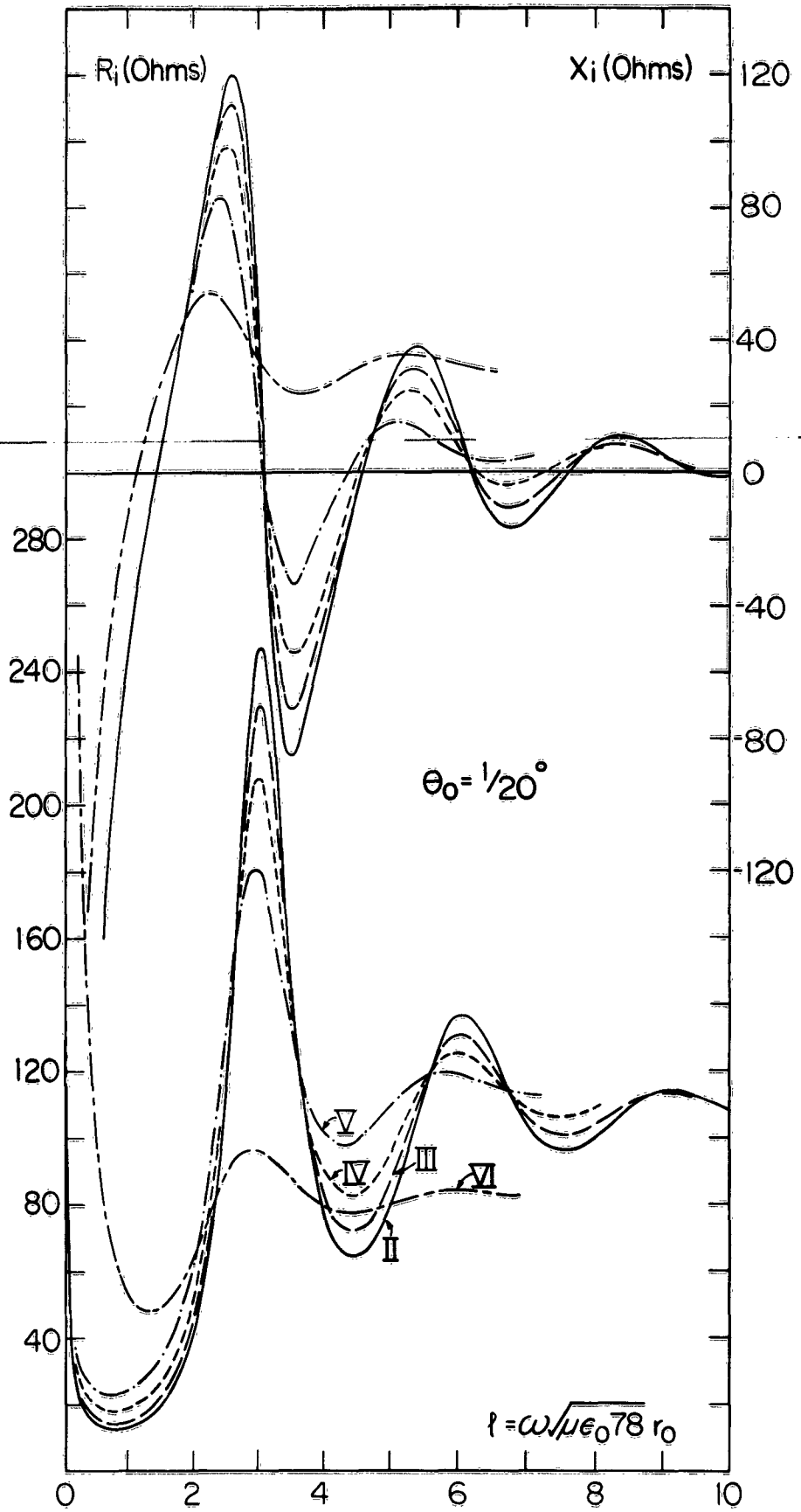

FIG. 3-5 θ_0 1/20°, MEDIA II TO VI. $Z_i = R_i + iX_i$, IN OHMS VS. $\ell = \omega\sqrt{\mu\epsilon_0}\,78\, r_0$. R_i : LEFT SCALE; X_i : RIGHT SCALE

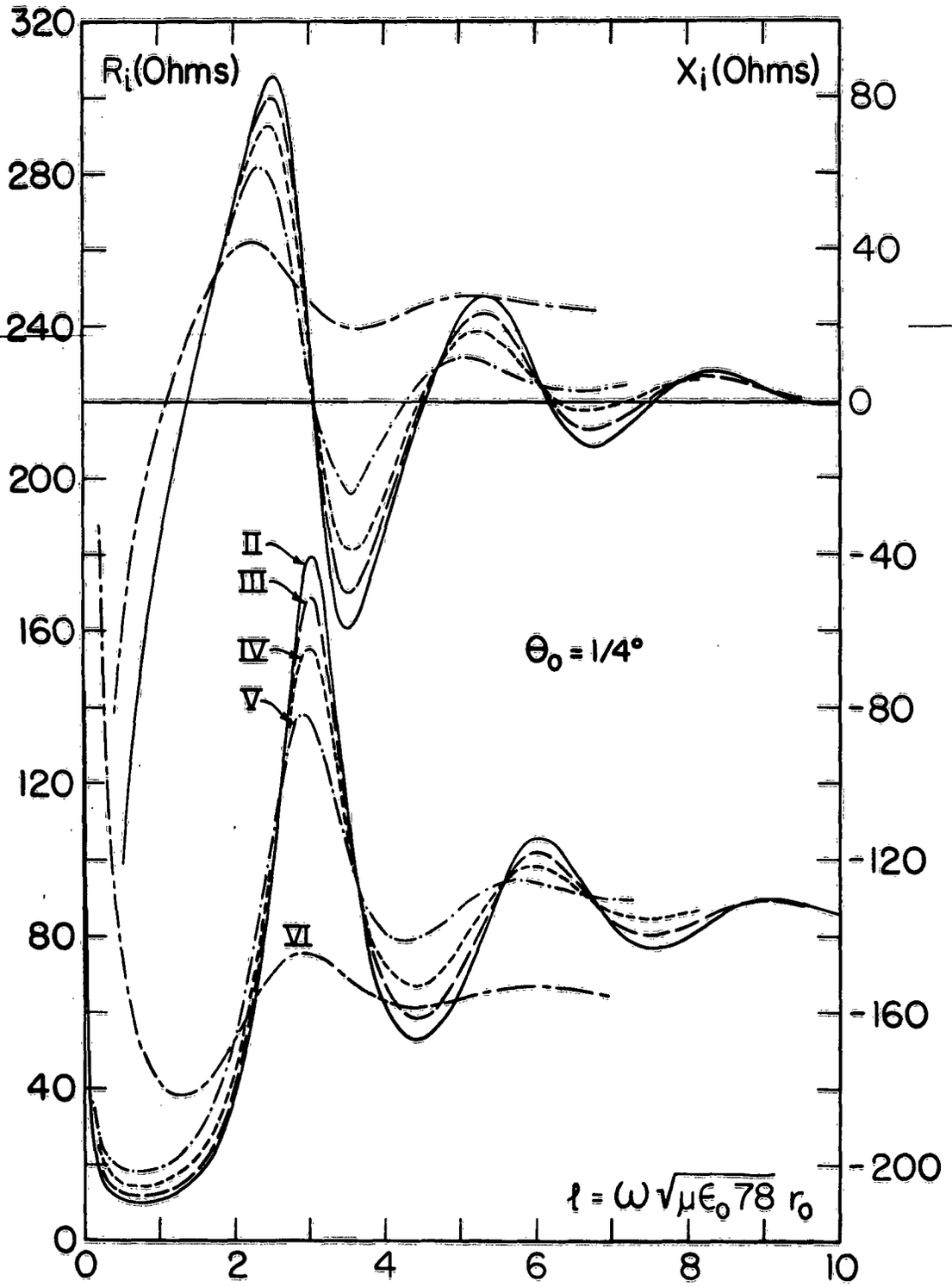

FIG. 3-6 $\Theta_0 = 1/4°$, MEDIA II TO VI. $Z_i = R_i + iX_i$ IN OHMS VS. $\ell = \omega\sqrt{\mu\epsilon_0 78}\, r_0$. R_i : LEFT SCALE, X_i : RIGHT SCALE

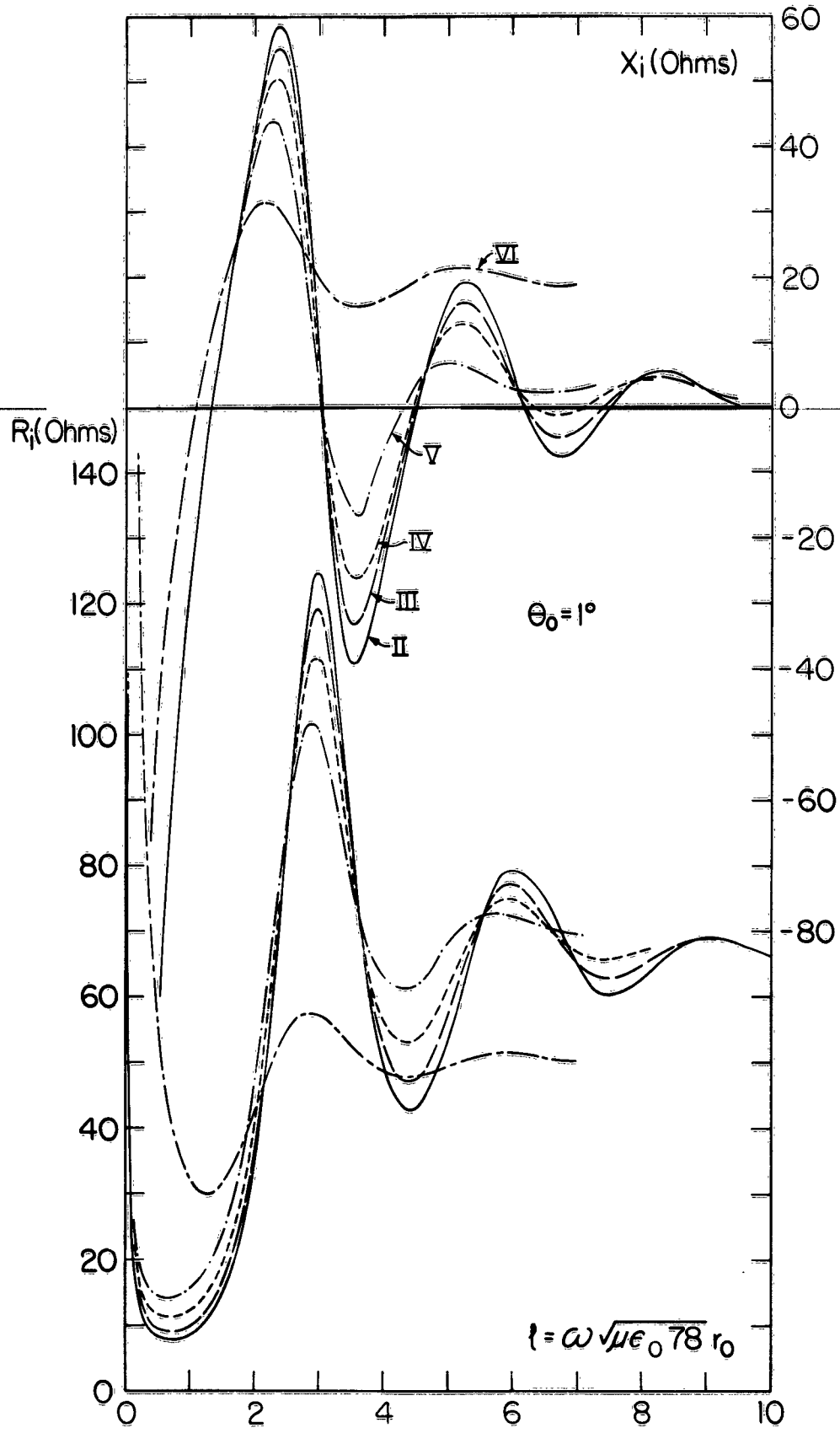

FIG. 3-7 $\theta_0 = 1°$, MEDIA II TO VI. $Z_i = R_i + iX_i$ IN OHMS VS. $\ell = \omega\sqrt{\mu\epsilon_0 78}\, r_0$. R_i : LEFT SCALE; X_i : RIGHT SCALE.

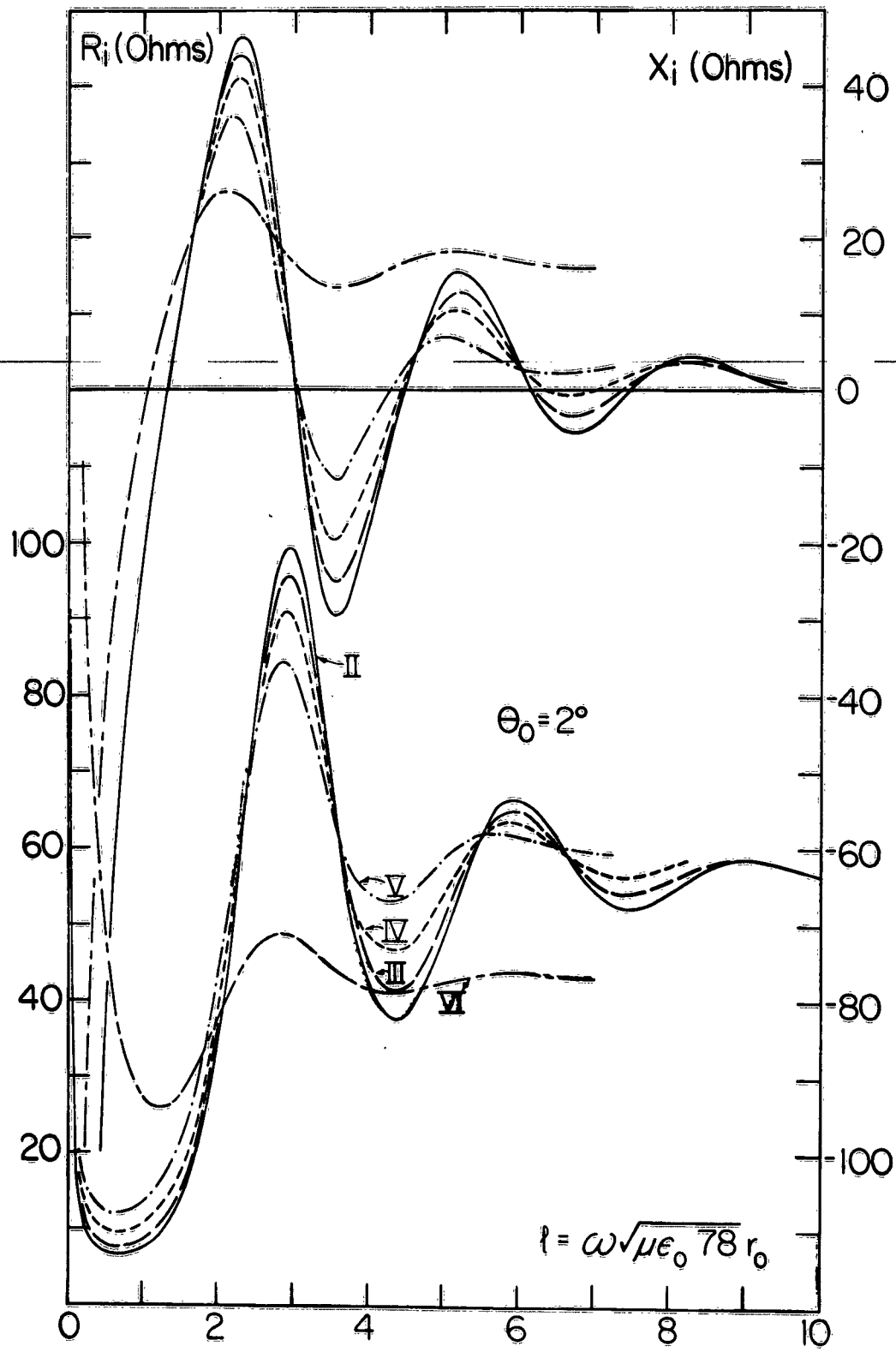

FIG. 3-8 $\theta_0 = 2°$, MEDIA II TO VI. $Z_i = R_i + iX_i$ IN OHMS VS. $\ell = \omega\sqrt{\mu\epsilon_0}\,78 r_0$. R_i : LEFT SCALE, X_i : RIGHT SCALE

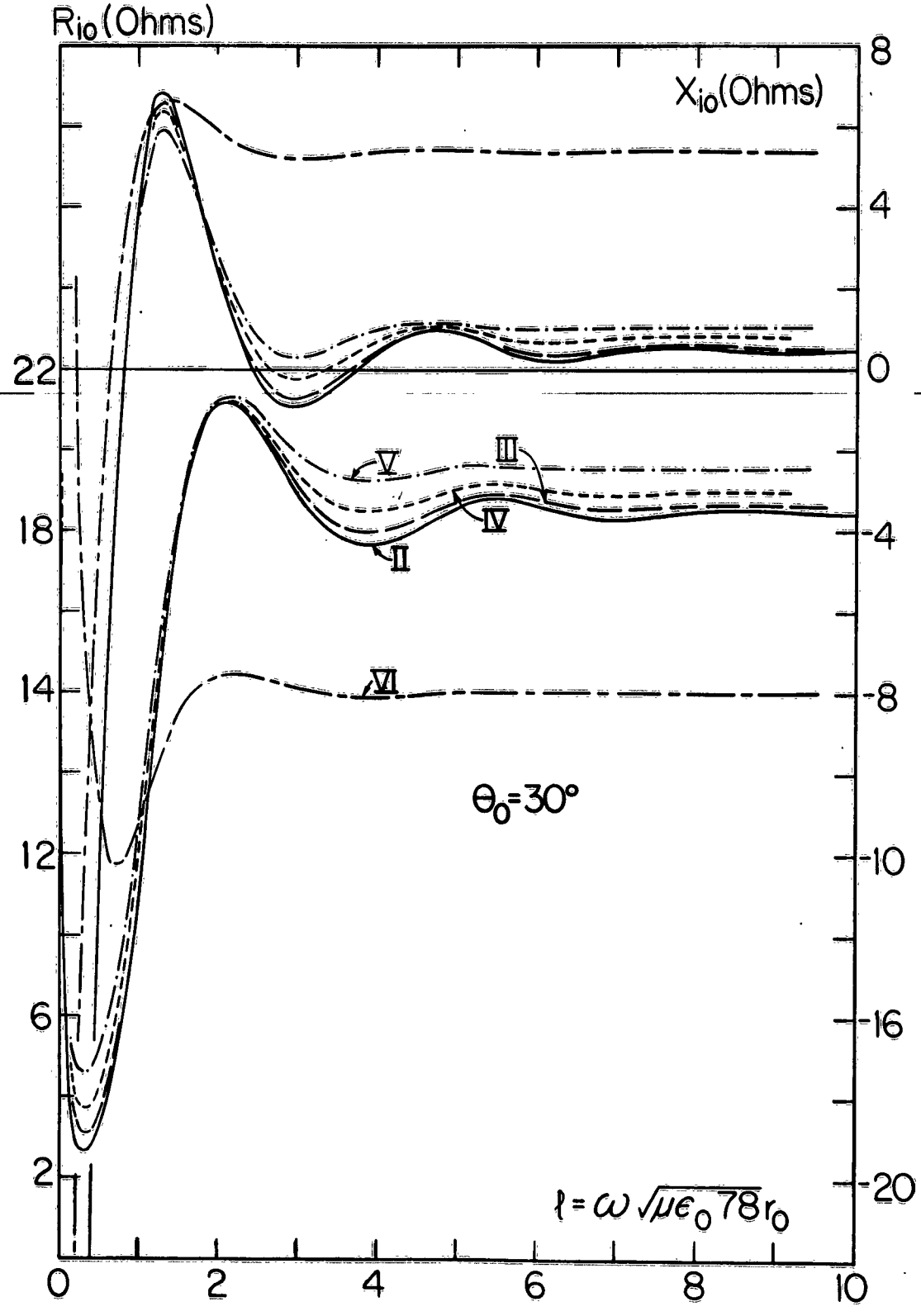

FIG. 3-9 $\theta_0 = 30°$, MEDIA II TO VI. $Z_{io} = R_{io} + iX_{io}$ IN OHMS VS. $\ell = \omega\sqrt{\mu\epsilon_0}\,78 r_0$ R_{io}: LEFT SCALE, X_{io}: RIGHT SCALE

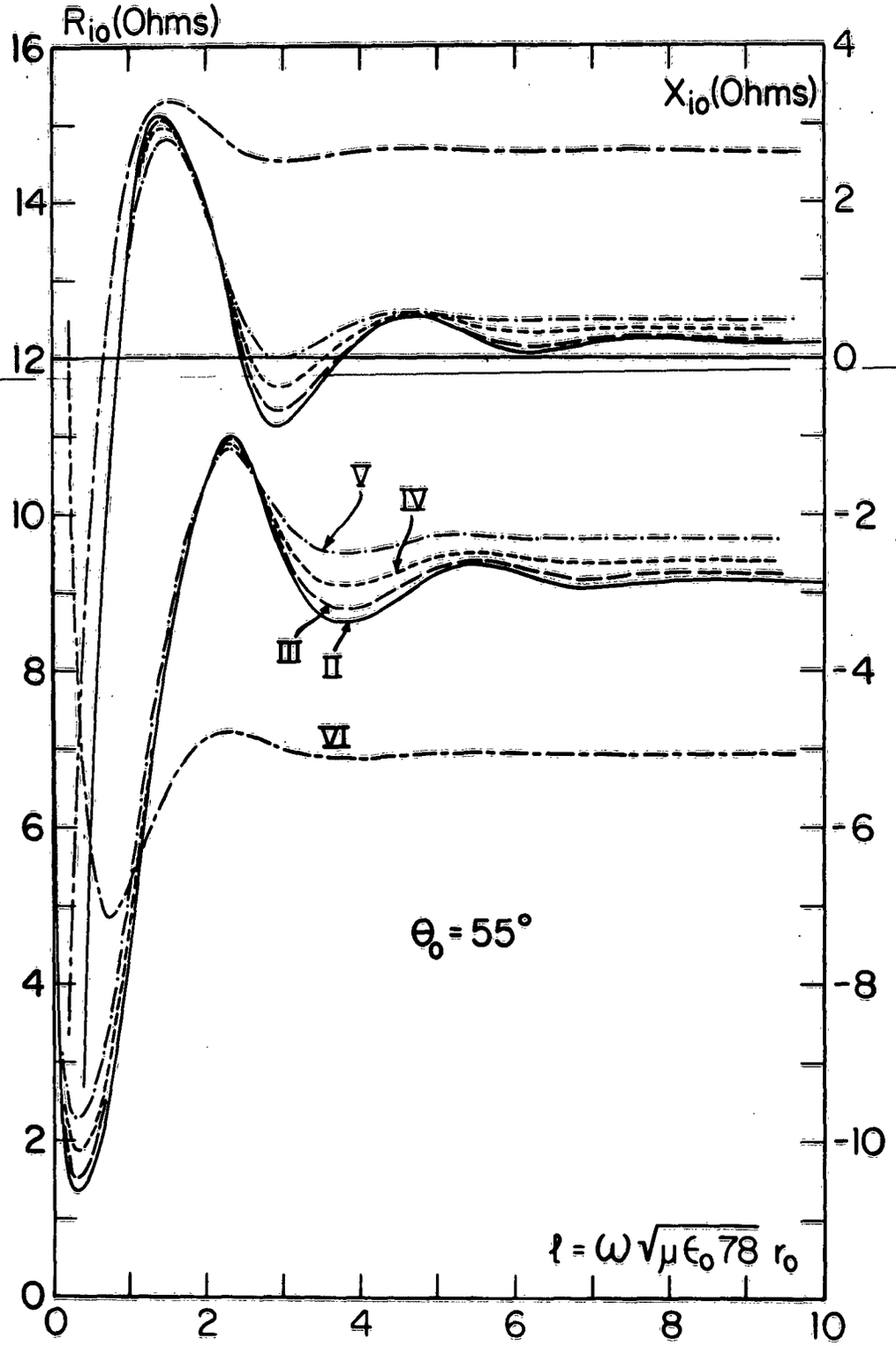

FIG. 3-10 $\theta_0 = 55°$, MEDIA II TO VI. $Z_{io} = R_{io} + iX_{io}$ IN OHMS VS. $\ell = \omega\sqrt{\mu\epsilon_0}\,78 r_0$. R_{io}: LEFT SCALE; X_{io}: RIGHT SCALE

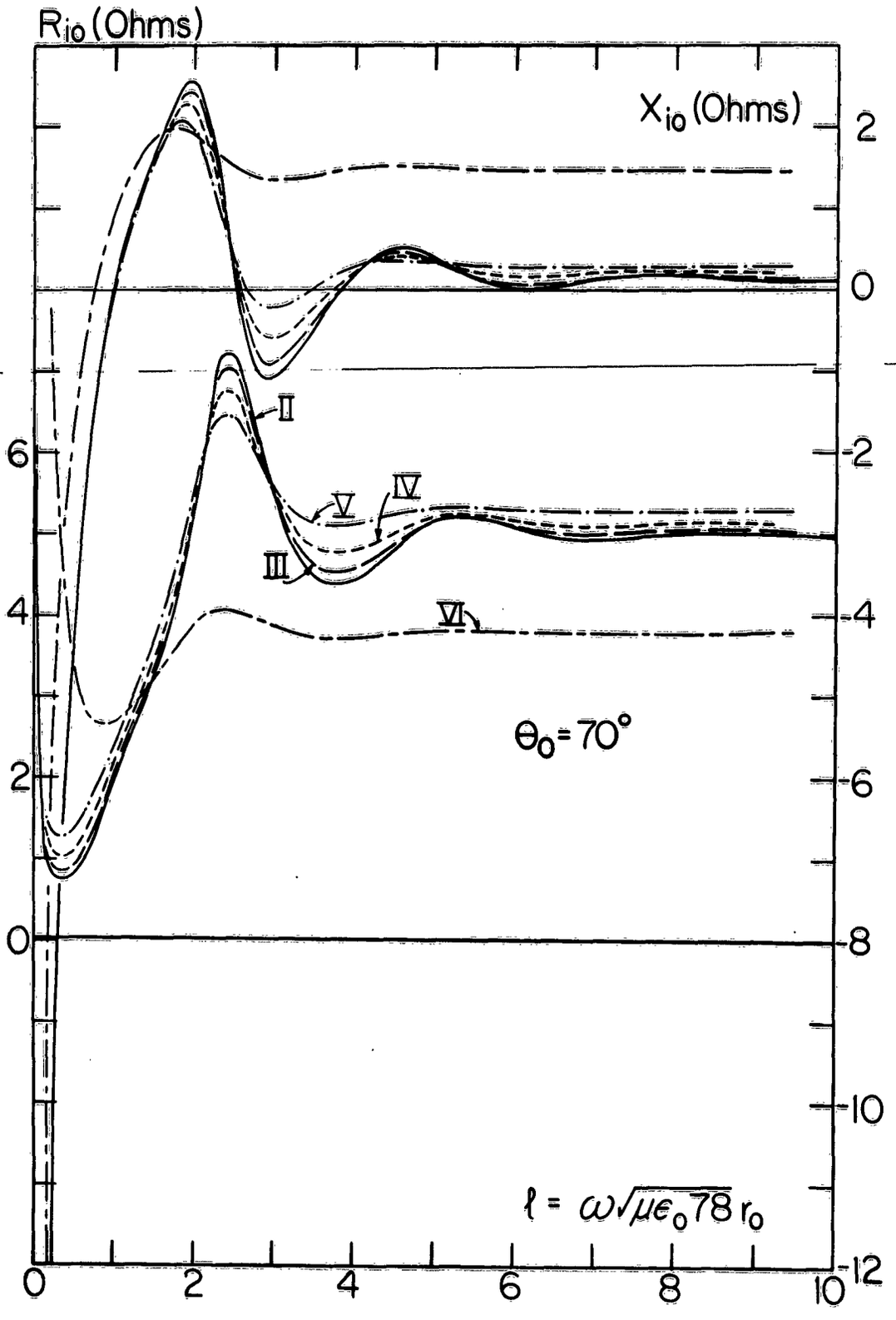

FIG. 3-11 $\theta_0 = 70°$, MEDIA II TO VI. $Z_{io} = R_{io} + iX_{io}$ IN OHMS VS. $\ell = \omega\sqrt{\mu\epsilon_0 78}\, r_0$. R_{io}: LEFT SCALE; X_{io}: RIGHT SCALE

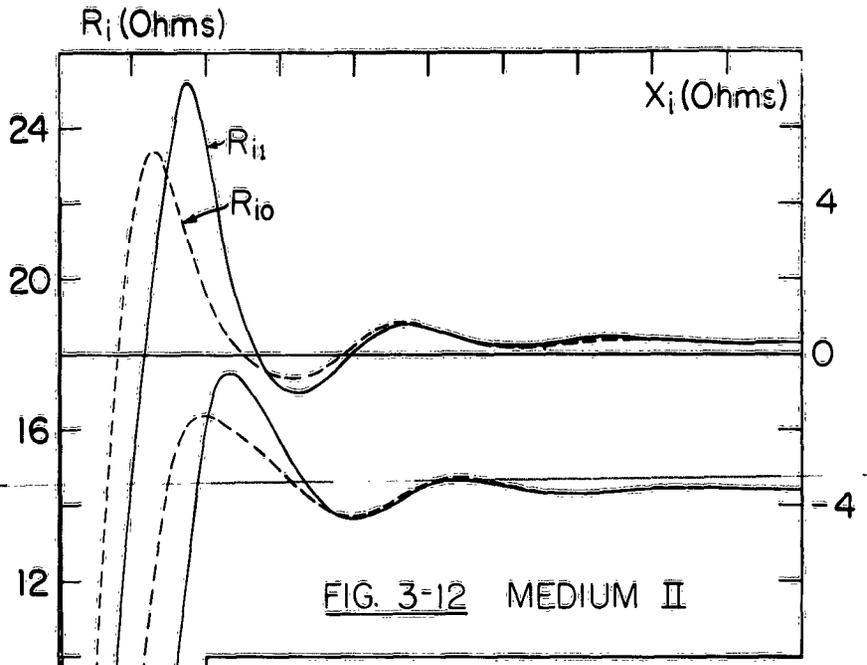

FIG. 3-12 MEDIUM II

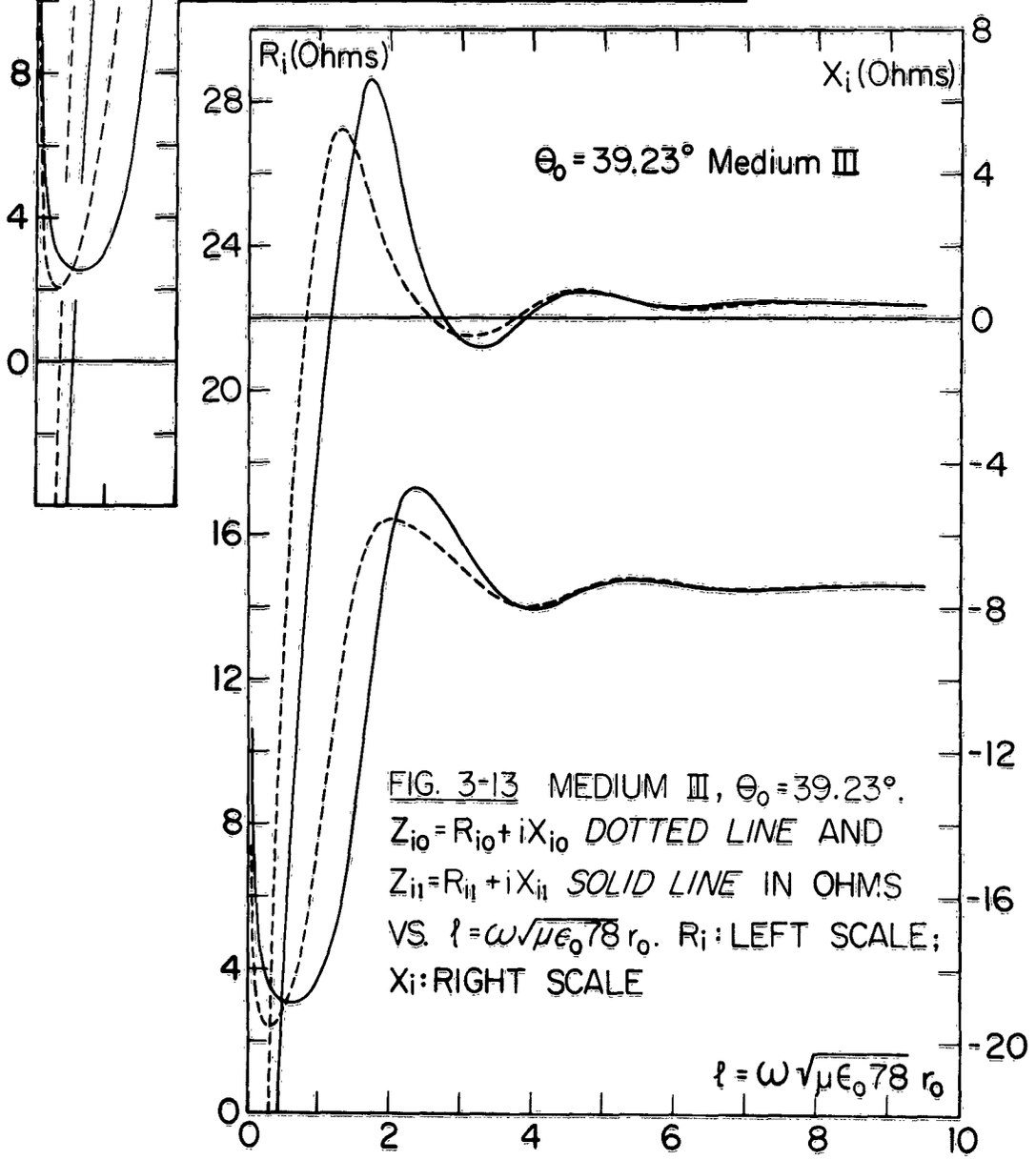

FIG. 3-13 MEDIUM III, $\Theta_0 = 39.23°$.
$Z_{io} = R_{io} + iX_{io}$ *DOTTED LINE* AND
$Z_{i1} = R_{i1} + iX_{i1}$ *SOLID LINE* IN OHMS
VS. $\ell = \omega\sqrt{\mu\epsilon_0 78}\, r_0$. R_i : LEFT SCALE;
X_i : RIGHT SCALE

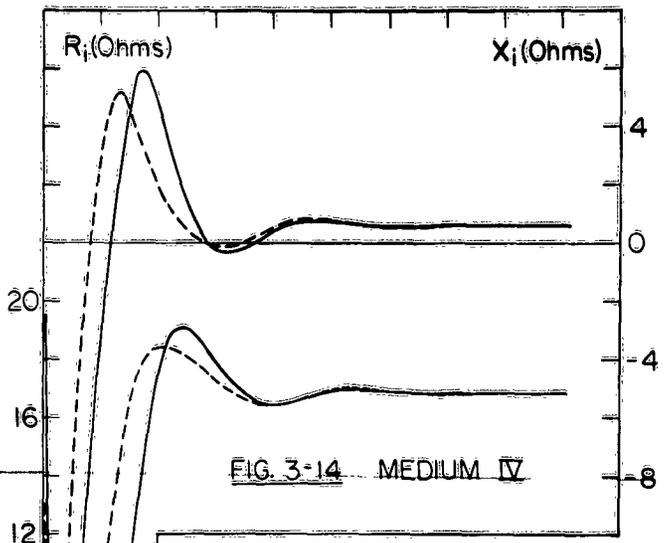

FIG. 3-14 MEDIUM IV

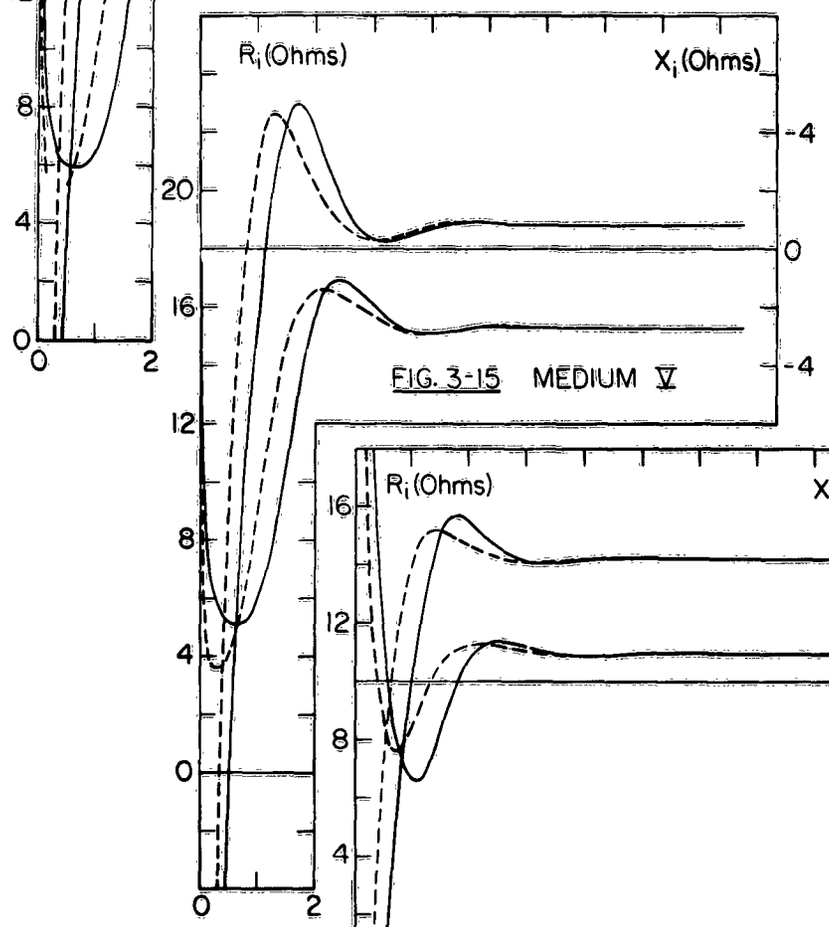

FIG. 3-15 MEDIUM V

FIG. 3-16 MEDIUM VI, $\theta_0 = 39.23°$
$Z_{i0} = R_{i0} + iX_{i0}$ *DOTTED LINE* AND
$Z_{i1} = R_{i1} + iX_{i1}$ *SOLID LINE* IN OHMS
VS $\ell = \omega\sqrt{\mu\epsilon_0}\,78\,r_0$. R_i: LEFT SCALE;
X_i: RIGHT SCALE

Activity Supply Officer
Building 1306, Charles Wood Area
Fort Monmouth, New Jersey (50)
Attn: Director of Research

Commanding Officer
Office of Naval Research
Navy 100, Box 39 (25)
Fleet Post Office
New York, New York

Armed Services
Technical Information Agency
Arlington Hall Station (10)
Arlington 12, Virginia
Attn: TIPDR

The Director
Naval Research Laboratory
Washington 25, D. C. (6)
Attn: Technical Information Office

Commander, AF CRL
AFRD, ARDC, CRRLC
Laurence G. Hanscom Field (6)
Bedford, Massachusetts
Attn: Electronics Research Directorate

Commanding General
Air Research and Development Command
P. O. Box 1395 (3)
Baltimore 3, Maryland
Attn: RDTRRP

Chief of Naval Research
Department of the Navy (2)
Washington 25, D. C.
Attn: Dr. A. Shostak, Code 427

Chief of Naval Research
Department of the Navy (2)
Washington 25, D. C.
Attn: Code 427

Commanding Officer
Office of Naval Research
495 Summer Street (2)
Boston, Massachusetts

Chief, Bureau of Ships
Department of the Navy (2)
Washington 25, D. C.
Attn: Code 810

Director, Air University
Library (2)
Maxwell Air Force Base
Alabama

Chief of Naval Research
Department of the Navy
Washington 25, D. C.
Attn: Code 421

Commanding Officer
Office of Naval Research
495 Summer Street
Boston, Massachusetts

Commanding Officer
Office of Naval Research
John Crerar Library Building
86 East Randolph Street
Chicago 1, Illinois

Commanding Officer
Office of Naval Research
346 Broadway
New York 13, New York

Commanding Officer
Office of Naval Research
1030 East Green Street
Pasadena, California

Commanding Officer
Office of Naval Research
1000 Geary Street
San Francisco 9, California

Head, Document Section
Technical Information Division
Naval Research Laboratory
Washington 25, D. C.

Martin A. Garstens
Magnetism Branch, Code 6430
Solid State Division
Naval Research Laboratory
Washington 25, D. C.

Commanding Officer
U.S.N. Air Development Center
Johnsville, Pennsylvania
Attn: NADC Library

Commander
U. S. N. Air Development Center
Johnsville, Pennsylvania
Attn: AAEL

Chief, Bureau of Aeronautics
Department of the Navy
Washington 25, D. C.
Attn. EI-1

Engineering Librarian
Convair
San Diego 12, California

Dr. John E. Pippin
Applied Physics and Ferrite Devices
Sperry Microwave Electronics Co.
P. O. Box 1828
Clearwater, Florida

Engineering Library
Sperry Microwave Electronics Co.
Clearwater, Florida

Dr. Lajos Rimai
Research Division
Raytheon Company
Waltham 54, Massachusetts

Elizabeth Weeks, Librarian
Raytheon Company
28 Seyon Street
Waltham 54, Massachusetts

Report Librarian
Sylvania Electric Products Inc.
Electronic Systems Division
100 First Avenue
Waltham, Massachusetts

Document Control Center
Wayland Library
Raytheon Manufacturing Co
Wayland, Massachusetts

J. E. Goldman
Scientific Laboratory
Ford Motor Company
Engineering Staff
P. O. Box 2053
Dearborn, Michigan

Charles C. H. Tung
Bell Telephone Labs
Murray Hill, New Jersey

Librarian
RCA Laboratories
Princeton, New Jersey

Dr. A. Amith
RCA
Princeton, New Jersey

Commander (2)
U. S. Naval Electronics Lab.
San Diego, California

Commanding General, RCBW
Rome Air Development Center
Griffiss Air Force Base (3)
Rome, New York

Commanding General
Air Research and Development Command
P. O. Box 1395 (2)
Baltimore, Maryland
Attn: RDDDE

Commander
Air Force Cambridge Research Labs.
Laurence G. Hanscom Field (2)
Bedford, Massachusetts
Attn: CROTLS

Commander
Wright Air Development Center
Wright Patterson Air Force Base
Ohio (2)
Attn. WCLRA Library

National Security Agency
Physical Sciences Division (2)
Fort George Meade, Maryland
Attn: Dr. Alvin Mackler

Associate Prof. A. Kaprielian
Department of Electrical Engineering
University of Southern California
University Park
Los Angeles 7, California

Assistant Secretary of Defense
(Research and Development)
Research and Development Board
Department of Defense
Washington 25, D. C.

Chief of Naval Operations
Department of the Navy
Washington 25, D. C.
Attn: Op-20

Chief of Naval Operations
Department of the Navy
Washington 25, D. C.
Attn: Op-32

Chief of Naval Operations
Department of the Navy
Washington 25, D. C.
Attn: Op-413

Chief, Bureau of Aeronautics
Department of the Navy
Washington 25, D. C.
Attn: EI-6

Technical Library
U. S. Naval Proving Ground
Dahlgren, Virginia

Director
Naval Ordnance Laboratory
White Oak, Maryland

Librarian
U. S. Naval Post Graduate School
Monterey, California

Air Force Office of Scientific Research
Air Research and Development Command
Washington 25, D. C.
Attn. SRY, Physics Division

Commanding General
Rome Air Development Center
Griffiss Air Force Base
Rome, New York
Attn: RCREC-4C

Commanding General
Rome Air Development Center
Griffiss Air Force Base
Rome, New York
Attn: RCR

Commander
Air Force Cambridge Research Center
230 Albany Street
Cambridge 39, Massachusetts
Attn: CRZJ

Commander
Air Force Cambridge Research Center
230 Albany Street
Cambridge 39, Massachusetts
Attn: CRZM

Commander
AF Cambridge Research Laboratories
Laurence G. Hanscom Field
Bedford, Massachusetts
Attn: Dr. Hollingsworth

Commander
Wright Air Development Center
Wright Patterson Air Force Base
Ohio Attn: WCRR

Sandia Corporation
Org. 1414, Sandia Base
Albuquerque, New Mexico
Attn: Dr. C. W. Harrison, Jr.

Sandia Corporation
Sandia Base
Albuquerque, New Mexico
Attn: Library Division 1912-1

Mr. Robert Turner
General Electric Company
Advanced Electronics Center
Cornell University
Ithaca, New York

Library
Airborne Instruments Lab
Walt Whitman Road
Melville, Long Island, New York

Secretary, Working Group
Semiconductor Devices
346 Broadway, 8th Floor
New York 13, New York
Attn: AGET

Metals Research Laboratories
Electro Metallurgical Company
Box 900, Niagra Falls, New York
Attn. Mr. R. J. Gladieux

Librarian
General Electric Research Lab.
P. O. Box 1088
Schenectady, New York

Westinghouse Electric Corp.
Research Laboratories
Beulah Road, Churchill Boro.
Pittsburgh 35, Pennsylvania

Prof O. E. H. Rydbeck
P. O. Box 456
Belmar, New Jersey

Dr. Melvin W. Aarons
811 East Genesee Street
Fayetteville, New York

Laboratory
Airborne Instruments
Mineola, New York

Commander
Wright Air Development Center
Wright Patterson Air Force Base
Ohio
Attn: WCRRM

Commandant
Air Force Institute of Technology
Wright Patterson Air Force Base
Ohio
Attn: MCLI Library

AF Special Weapons Center
Kirtland Air Force Base
Albuquerque, New Mexico
Attn. SWOI

Headquarters
AF Missile Test Center
MU-135, ARDC
Patrick Air Force Base
Florida

U. S. Coast Guard
1300 E Street, N. W.
Washington 25, D. C.
Attn: EEE

M. A. Krivanek, Chief
Systems Component Branch
Electronic Warfare Division
Signal Corps Agency
White Sands Proving Ground
New Mexico

Mr. A. D. Bedrosian
Signal Corps Liaison Office
Mass. Institute of Technology
Building 26, Room 131
Cambridge 39, Massachusetts

Chief, European Office
ARDC Command
Shell Building
60 Rue Ravenstein
Brussels, Belgium

Dr. J. Anton Hedman
Ordnance Materials Res. Office
Watertown Arsenal
Watertown, Massachusetts

Acquisitions Officer
ASTIA Reference Center
Arlington Hall Station
Arlington 12, Virginia

Stanford Research Institute
Documents Center
Menlo Park, California
Attn: Mary Lou Fields

Dr. C. H. Papas
Dept. of Electrical Engineering
California Institute of Technology
Pasadena, California

Stanford Electronics Lab
Stanford University
Stanford, California
Attn. Document Library
Applied Electronics Lab.

Department of Electrical Engineering
Yale University
New Haven, Connecticut

Librarian
Johns Hopkins University
3313 St. Paul Street
Baltimore 1, Maryland

Radiation Laboratory
Johns Hopkins University
3315 St. Paul Street
Baltimore 1, Maryland

Director, Lincoln Laboratory
Mass. Institute of Technology
Bedford, Massachusetts

Mr. John Hewitt
Document Room
Research Lab. of Electronics
Mass. Institute of Technology
Cambridge 39, Massachusetts

Professor A. Von Hippel
Mass. Institute of Technology
Lab. for Insulation Research
Cambridge 39, Massachusetts

Library, Room A 229
Lincoln Laboratory
P. O. Box 73
Lexington 73, Massachusetts

R. H. Siegel, Head
Theory and Analysis Department
Willow Run Laboratories
University of Michigan
Willow Run Airport
Ypsilanti, Michigan

Librarian
National Bureau of Standards Library
Room 301, Northwest Building
Washington 25, D. C.

Librarian
U. S. Department of Commerce
National Bureau of Standards
Boulder, Colorado

Dr. Earl Callen
National Security Agency
Physical Sciences Division
Fort George Meade, Maryland

Dr. H. Campaigne
National Security Agency
Physical Sciences Division
Fort George Meade, Maryland

Chung Kung University
Electrical Engineering Department
Taiwan, Taiwan
Republic of China
Attn: Professor Chao-Nei Cuan
Head, Eng. Department

Mr. D. S. Jones
Department of Mathematics
Univ. College of No. Staffordshire
Keele, Staffordshire, England

Professor Paul Rene Mito
Osaka City University
Dept. of Engineering Sciences
14 Nishi Ogimachi Kitaku
Osaka, Japan

Donald C. Stinson
Dept. of Electrical Engr.
University of Arizona
Tucson 25, Arizona

Professor Jerome B. Singer
Div. of Electrical Engineering
University of California
Berkeley 4, California

Professor Charles Kittel
Department of Physics
University of California
Berkeley 4, California

Serials Library
Brandeis University
Waltham, Massachusetts

Professor H. G. Booker
School of Electrical Engineering
Cornell University
Ithaca, New York

Library, College of Engineering
University Heights Library
University Heights
New York University
New York 53, New York

E. A. Chapman, Librarian
Rensselaer Polytechnic Institute
Amos Eaton Hall
Troy, New York

Robert Plonsey
Department of Engineering
Case Institute of Technology
University Circle
Cleveland 6, Ohio

Dept. of Electrical Engineering
Case Institute of Technology
University Circle
Cleveland 6, Ohio
Attn. S. Besly, Head

Dr. C. J. Falkenbach
Battelle Memorial Institute
Columbus, Ohio
Attn: Electrical Engineering Division

Librarian
Engineering Library
Brown University
Providence, Rhode Island

Professor A. W. Straiton
Dept. of Electrical Engineering
University of Texas
Austin 12, Texas

Mr. William Way
Research Librarian
Technical Instruments Corp.
3349 Cahuenga Boulevard
Hollywood 28, California

SOLID STATE ONLY

Martin A. Garstens, Head
Paramagnetic Section
Magnetism Branch
Solid State Division
Naval Research Laboratory
Washington 25, D. C.
Attn: Code 6451

Dr. Reimer Bouwkamp, Jr.
Ordnance Materials
Research Laboratory
Watertown Arsenal
Watertown, Massachusetts

Mr. A. Saiba
Himeji Technical College
Himeji, Japan

Electronics Research Laboratory
Division of Electrical Engineering
University of California
Berkeley 4, California
Attn: Librarian

Johns Hopkins University
34th and Charles Street
Whitehead Hall
Baltimore 18, Maryland
Attn: Mr. J. O. Artman

Librarian
Physics Department
Amherst College
Amherst, Massachusetts
Attn. Mr. Romer

Professor I. Lowe
Department of Physics
University of Minnesota
Minneapolis, Minnesota

Professor R. E. Norberg
Department of Physics
Washington University
St. Louis, Missouri

Microwave Research Institute
Polytechnic Institute of Brooklyn
55 Johnson Street
Brooklyn, New York
Attn: Librarian

Dr. Sidney Shapiro
Arthur D. Little, Inc.
19 Acorn Park
Cambridge 40, Massachusetts

Dr. Simon Foner
Lincoln Laboratories
Box 73
Lexington, Massachusetts

Mr. William H. Frost
Ewen Knight Corporation
226 A Street
Needham, Massachusetts

Dr. Edward U. Condon
6304 Waterman Avenue
St. Louis, Missouri

Dr. W. M. Walsh
Bell Telephone Labs., Inc.
Murray Hill, New Jersey

Librarian
IBM Watson Laboratories
612 West 115th Street
New York 27, New York

ELECTROMAGNETIC RADIATION ONLY

Michigan State College
Department of Mathematics
East Lansing, Michigan

Microwave Research Institute
Polytechnic Institute of Brooklyn
55 Johnson Street
Brooklyn, New York

Mr. L. E. Swarts, Jr.
Building 12, Room 2617
Hughes Research Laboratories
Culver City, California

Professor O. E. H. Rydbeck
P. O. Box 456
Belmar, New Jersey

One Copy Unless Otherwise Specified